1957

Ship model bending moments in waves

Lutzi, Philip C.; Kimball, Edwin D.

Massachusetts Institute of Technology, 1957.

http://hdl.handle.net/10945/24832

SHIP MODEL BENDING MOMENTS IN WAVES

Philip C. Lutzi
and
Edwin D. Kimball

SHIP MODEL BENDING MOMENTS

IN WAVES

by

PHILIP C. LUTZI, Lieutenant, U. S. Coast Guard

B.S., U.S. Coast Guard Academy

(1951)

and

EDWIN D. KIMBALL, Lieutenant, U. S. Navy

B.S., Tufts College

(1950)

39

SUBMITTED IN PARTIAL FULFILLMENT

OF THE REQUIREMENTS FOR THE

DEGREE OF NAVAL ENGINEER

at the

MASSACHUSETTS INSTITUTE OF TECHNOLOGY

May 1957

Department of Naval Architecture and
Marine Engineering, May 20, 1957

Signature of Authors ______________________

____

Certified by ______________________
Thesis Supervisor

Accepted by ______________________
Chairman, Departmental Committee
on Graduate Students

ABSTRACT

SHIP MODEL BENDING MOMENTS IN WAVES

by

Philip C. Lutzi and Edwin D. Kimball

Submitted to the Department of Naval Architecture and Marine Engineering on May 20, 1957 in partial fulfillment of the requirements for the degree of Naval Engineer.

The objects of this thesis were 1) to investigate the bending moments induced in a model of a 32,000 ton deadweight tanker in regular waves from ahead, 2) to compare our results with and add to the data available on bending moments measured by model tests, and 3) to check the validity of the static bending moment calculation by comparing it with the results of the model tests. Within these objects we also wished to ascertain 1) that maximum bending moments do exist at the midships section, and 2) what the effect is of different loading conditions on the model bending moments.

The experimental data was obtained by fastening a flexure bar in the bottom of the tanker model, cutting the model at three sections (amidships, 10% of the length forward of amidships, and 10% of the length aft of amidships), and measuring the bending moments at these three cut sections by electrical resistance type strain gages mounted on the flexure bar and wired to Sanborn galvanometer pen type recorders. The model was towed at various constant towing forces in waves during these measurements.

The experimental data indicated that 1) the maximum absolute bending moments recorded in the wave conditions were well below the values obtained by the static calculation, 2) the maximum moment occurred at the amidships section, 3) for a given wave length, the speed (in the operating range of the ship) had small effect on the amidships bending moment, and 4) the ballast load condition investigated gave smaller bending moments than the full load condition. A maximum bending moment of 71.0 inch-pounds was obtained at the amidships section at a wave length of 1.5L and a speed of 0.82 knots (9.2 knots ship speed), and it was in the sagging condition.

Thesis Supervisor: Martin A. Abkowitz
Title: Associate Professor of Naval Architecture

TABLE OF CONTENTS

LIST OF FIGURES

Figure

LIST OF FIGURES (Continued)

LIST OF SYMBOLS

a	Wave height, in inches, or as a fraction of wave length
K_y	Radius of gyration, in inches or as a fraction of L.B.P.
L	Length between perpendiculars, in feet
T_e	Period of wave encounter, in seconds
T_p	Natural period of pitching, in seconds
V_s	Still water speed, in knots
V_v	Speed of ship or model in waves, in knots
V_w	Wave speed, in knots
λ	Wave length, in feet, or as a fraction of the model length

I. INTRODUCTION

This thesis was conducted with three purposes in mind. First, the authors desired to determine the bending moments induced in a model of a thirty-two thousand ton deadweight tanker in regular waves from ahead for various loading conditions. In order to try to resolve some of the differences between previous model bending moment tests, we wished to compare our results with, and add to, the few data available on bending moments measured by model tests. To give full meaning and usefulness to our results we must also compare them to the conventional static bending moment calculated by assuming the ship to be poised on a stationary wave of length equal to the ship length and of height equal to 1/20 of the length.

The provision of adequate longitudinal strength has always been an important problem in the design of steel ships. This phase of naval architecture has been brought to the forefront in recent years by the failure of longitudinal strength members in some tankers due to high longitudinal bending moments, by the advent of the large supertankers now being built up to 100,000 tons deadweight, and by the increasing speed of modern ships.

The problem of designing adequate longitudinal strength into ships may be considered in two parts as stated by Mr. E. V. Lewis in Reference (8). First is the determination of the loads acting on the ship, and second is the design of the ship to carry these applied loads. The first part consists of the

following:

1) determining the loads on the hull in calm water due to various cargo, fuel, and ballast loadings.
2) estimating the proportions of the waves encountered by ships at sea.
3) measuring the moments caused by these waves and loadings at various ship speeds.

The second part consists of finding the stresses resulting from the moments, and the scantlings required to limit the stresses to allowable values.

The second part of the problem has received far greater study than the first and will not be studied further in this thesis. We are concerned with items 1) and 3) of the first part of the problem. Item 2), the wave proportions, is a problem on which the oceanographers are currently compiling data. We used various regular waves but always kept the wave height 1/20 of the wave length, that is, constant wave slope.

In the field thus defined three model methods have been used to attack the problem. The first, described in Reference (8), employed a 4.79 foot T2-SE-A1 tanker model cut at amidships into two separate sections connected by flexure bars to give the required rigidity. The deflection of the stern relative to the bow section was measured by an electrical pickup installed between the stern and a rigid frame extended from the bow section. The deflections were converted to bending moments by the calibration procedure.

The second method made use of a 19.7 foot model made

of thin brass plate and constructed in nearly the same manner as an actual ship. It had symmetrical fore-and-aft bodies, a flat bottom, and vertical side walls. A strain gage measured the stress in the deck approximately at amidships. This can be readily converted to bending moment by a constant factor. The tests conducted and the results are described in Reference (3).

In the third method, explained in Reference (13), a 4.81 foot model of a passenger-cargo ship was cut transversely at the forward quarter point and amidships, and held together by an aluminum bar two inches wide by one-half inch thick by three feet long, mounted near the bottom of the model. The bending moment was measured at both sections by resistance type strain gage bridges mounted directly on the flexure bar. The method used in this thesis is similar to this last method because it was the least expensive, and it could be used where moments were to be taken at more than one station.

Our model (5.00 feet L.B.P.) was cut transversely at the amidships station and at ten percent of the length between perpendiculars forward and aft of the amidships station. Strain gage bridges mounted on the flexure bar at these three positions measured the bending moments which were recorded on Sanborn galvanometer pen type recorders. High speed motion pictures of the model runs gave the pitch and wave profiles. The regular installed equipment at the M.I.T. Ship Model Towing Tank was used to record the wave trace and the model speed.

Tests on the model were run at five towing forces (still water speeds), four wave conditions, and two loading conditions.

Both model test results and calculations are needed and should be used together in this area of investigation if we are to arrive at the true answers to our problem.

II. PROCEDURE

The model used for the tests in this project was that of a 32,000 ton deadweight tanker operated by the Holland-America Lines. The particulars are listed in Appendix A. The model was well hollowed out when received from Holland, with the side and bottom 0.75 inches thick. This can be seen well in Figure XVII. No additional removal of wood was required, and the bottom and sides were of uniform thickness.

The model was to be cut at three sections and held together with an aluminum bar. Aluminum was chosen for its light weight property. The bar was sized to give the largest possible strain gage elongations and to give the model a natural frequency of vertical two-noded vibration well above the highest period of encounter of the model in waves. The natural frequency of the vertical two-noded vibration of the model-bar combination was calculated using Reference (10) to get the water inertia effect, and Rayleigh's method as modified by Professor F. M. Lewis to get the frequency. Several sizes of bar were calculated to give the proper natural frequency and a one-half inch thick by one inch wide bar was chosen because it was readily available.

The natural frequency of the vertical two-noded vibration of the ship was calculated by the modified Schlick formula, as shown in Appendix B. This gave a frequency of 0.87 cycles per second for the ship or 9.76 cycles per second for the model. The one-half inch by one inch aluminum bar gave a calculated natural frequency of 8.00 cycles per

second. Upon test, when the model was made to pitch and then released, the natural frequency was measured from the strain gage record on the Sanborn Recorder and found to be 10.5 cycles per second in the full load condition and 10.0 cycles per second in the ballast condition. Since the actual natural frequency of the model corresponded very closely to that for the ship, any vibratory phenomena occurring in the ship, such as the effects of slamming, would be approximated closely in the model also.

A wood base three-quarters of an inch thick was glued and screwed to the inside of the model bottom to place the bar at the right height in the model, to give enough wood to screw down the bar adequately, and to provide space for the installation of the strain gages. The aluminum bar was drilled and screwed down in the model and the model was then cut transversely at the three designated sections on a circular saw. The bar was located approximately at the vertical center of the resistance forces on the model to eliminate any bending moment due to these resistance forces. These forces would cause only negligible moments.

After completing the cuts the bar was removed for installation of the strain gages. Four A-5 type strain gages were installed on the bar at each of the points corresponding with the cuts in the model, two on top and two on the bottom. This arrangement gives only vertical bending moments, eliminating any errors due to transverse bending, simple tension or compression, and changes in humidity or temperature as might

occur with only one gage at each section. The gages in each section were wired to make up a full bridge (see Figure XVI) to give the maximum sensitivity to strains as strains were expected of about one hundred micro-inches. The two wires from each gage were taken directly to the plug and connections made there, rather than at the gages, to facilitate checking or repair of the circuit in the event of trouble. The gages and adjacent leads were well covered with wax to waterproof them. The bar was then reinstalled permanently in the model.

The next problem was to install the weights to make the full load condition in the model as close as possible to the full load condition in the ship. As can be easily seen, that is rather difficult as the wood can be thinned down only so much. However the weight and longitudinal center of gravity of each of the four sections of the model did agree with the ship scaled down to model size. This was not entirely possible in the ballast condition, however it was very close to being right. The weights installed were small cast lead weights which could be easily shifted around for the different loading conditions and were each secured with a single screw to the bottom of the model.

Sealing the model at the cuts and deck edge was accomplished using electrical scotch tape with a small amount pushed in to the cuts to prevent the tape from restraining the bending of the model. This tape performed very well in the tests, however one mistake was made in this area in that the model sections were not completely varnished or painted after the

cuts were made to prevent any leakage water from soaking in and separating the lifts. This had to be done part way through the model tests.

At this point a few trial runs were made to check the behavior of the model in waves without measuring any moments. It was found necessary to build a shield to prevent water coming over the bow from splashing over the box around the amidships opening in the deck. This was made of thin sheet metal and, as the motion pictures show, was very effective. These trial runs were also used to align the tape on the upper towing wire so that it tripped the electric eye installed near the middle of the tank at the same time that the vertical bar on the towing bracket coincided with the middle vertical white tape across the two horizontal reference bars in the middle of the tank. By this method we were able to get a reference point both on the Sanborn Recorder paper and the motion picture film. This enabled us to later determine the wave profile and position of the ship at the time of the maximum bending moment.

The radius of gyration was determined by the following method. The model was suspended from two springs of equal spring constant at equal distances from the center of gravity. It was made to oscillate in air first in pitching and then in heaving and the time for thirty cycles in each case was measured by stop watch. From these figures the radius of gyration was calculated to be 0.212 L.B.P. for full load condition and 0.223 L.B.P. for ballast condition as shown in

Appendix B. To determine the natural pitching period the model was made to oscillate in the tank in pitch in what seemed to be the natural frequency and released. The natural period was then measured from the Sanborn Recorder tape by averaging several cycles.

The method of transmission of the strain gage currents from the model to the shore requires some description. Since no carriage is available in the M.I.T. tank it was necessary to use a "fish pole" to lead the wires to the edge of the tank. This fish pole required someone to walk down the tank as the model made each run, and close attention was required to see that no tension was put on the wires which would introduce errors in the strain gage readings. The strain gage readings were very sensitive to any movements of the lead in wires or fish pole so that considerable effort was made to hold the fish pole so that the lead in wires would be in the same position relative to the model whenever it was run and whenever a zero reading was taken on the recorders for a run. Considerable more certainty as to the accuracy of the strain gage readings would be possible if a carriage were available in the tank. Inaccuracies from this cause may be large for individual runs but are small for a whole curve in our results, as the curves seem to indicate the proper trends. Besides errors in the strain gage readings the fish pole procedure may easily introduce errors in the speed of the model in waves. We experienced this as we measured different model speed in waves as different people operated the fish pole on identical runs.

However, the fish pole procedure appears to be the best method for transmitting electrical quantities from the model to the shore until such time as a carriage is available.

The wires into the model consisted of twelve wires grouped into three cables, one for each strain gage bridge. These were connected to the leads in the model by two Jones plugs, bridges numbers one and two on one plug, and bridge number three on another plug. The "shore" end of the wires were taken to Sanborn Recorders. A four-channel Sanborn Recorder was available on the floor above the tank, but it was not desirable in this case to use it, because it would have required an additional person and the use of telephones in order to make our runs. Also that recorder was available very little of the time. However it would have simplified the problem of synchronizing the tapes from the two recorders used. One two-channel Twin Viso Sanborn Strain Gage Recorder Model 60-1300, and one single-channel Sanborn Strain Gage Recorder Model 151-100A were used to record the strains in the model, and were placed at the dynamometer end of the towing tank with the other tank instruments. The man at this end of the tank operated both the strain gage recorders and the tank instruments.

The tank instruments used in these tests consisted of the following:

1) the speed measuring equipment including the Eput meter, the oscillator, the integrator, and the single-channel Sanborn Recorder,

2) the single-channel Sanborn Recorder used to measure the wave heights from the variable capacitance probe output,

3) the towing dynamometer, and

4) the wave making apparatus.

The operation of these is well described in Reference (2), as is the tank itself.

The calibration of the strain gage bridges was accomplished in the following manner. The model was clamped to a solid desk with the forward two sections overhanging the desk. A wire was led from a screweye on the bow over a pulley secured to the ceiling and down to a weight pan. After balancing the recorders and establishing a convenient zero, weights were added to the pan in small increments and the moments recorded by the recorder. The moments of the weights were plotted against the strain gage readings on the 5x scale of the recorder to give the calibration curves for sections 1 and 2. The model was turned around so that the after section was overhanging and the procedure repeated using section 3 bridge. The slopes of these curves were used as the factors to convert the strain gage readings to the bending moments throughout the runs. This set up can be seen in Figure XXI. These calibrations were repeated twice during the runs and at the completion of the runs, and remained practically constant indicating that the strain gages did not drift or change calibration. The resistance to ground remained above the minimum value throughout the tests.

With the calibration complete we now turn to the sequence followed in conducting the actual tests. First the model was run in still water to get the towing weights on both dynamometer pans to give us the four still water speeds desired. These were (1) slightly above design speed, (2) design speed, (3) about 0.8 of design speed, and (4) about 0.6 of design speed. The wave maker was then set to give the desired wave by use of the calibration curve in the tank for the wave length and the wave height recorder for the wave height. Then the five runs, zero speed and the four mentioned before, were conducted before changing to another wave.

Each run was conducted in the following manner. After allowing the tank to calm down from the previous run, the wave maker was started by the man at the dynamometer end of the tank after establishing zero on the strain gage recorders. The model was started down the tank by the man at the dynamometer end when the waves reached the beach at the far end of the tank. The man with the fish pole carefully followed the model down the tank. As the model approached the center of the tank, the man operating the movie camera turned on the floodlights, gave the man at the dynamometer end of the tank the signal to push the marker switch used to synchronize the two recorder tapes, and prepared to take the pictures. The manualmarker switch was required to synchronize the recorder tapes because the signal from the electric eye could only be fed into one of the recorders due to the electrical differences in the recorders, which made it impossible to connect the

electric eye signal into both recorders without blowing fuses. As the model passed through the middle of the tank the motion pictures were taken and the electric eye signal was recorded on the strain gage tapes. The model was allowed to run about one-half of the remaining distance in the tank and then stopped by the man at the instrument end of the tank, as the full length of the tank was not usually required to get our readings. The water was allowed to calm down and another zero taken on the strain gage recorders before returning the model to the other end of the tank for the next run.

The recorder tapes and the motion pictures were synchronized by the electric eye and the white tape on the reference bars as mentioned before. However synchronizing the two recorder tapes was accomplished by transferring the distance between the manual marker signal and the electric eye signal on the two-channel strain gage recorder to the tape from the one-channel strain gage recorder and marking it off from the manual marker trace on the latter tape in the right direction. The manual marker trace on the two tapes and the electric eye marker on the two-channel tape (arrow) can be seen in Figure XXIII.

The dynamic bending moments measured from the recorder tapes and reported in this thesis are the average of the five highest peaks in each case, discounting obviously erratic points. This was felt to be the most rational procedure giving more reasonable information than would the single highest peak or the average of all the peaks.

After each five runs the wave maker was adjusted to give another wave condition and five more runs conducted. All the runs in the full load condition (26) were conducted first, after which the weights in the model were changed to give the ballast condition. The radius of gyration and the natural pitching period were obtained before proceeding with the test runs in the same manner as for the full load condition. 26 runs were conducted in the ballast condition. The data for these runs is listed in Appendix D. After each run the model was checked for water and removed if present. It was originally intended to test the model in more conditions of loading but due to the trouble experienced with the lifts of the model separating when they got wet and the difficulties in the time schedule of the towing tank, it was only possible to test the model in two conditions of loading.

III. RESULTS

The results of the bending moment test of the model are presented in the following graphs.

Figure I - Total bending Moment vs. Model Speed at Full Load. This graph considers only the midship section, and a wave condition of $\lambda = L$ and $a = \lambda/20$. Conventional static calculated bending moments in hogging and sagging, as supplied by the ship owner and converted to model size, were also plotted. The Smith effect is not included in these conventional static bending moment values.

Figure II - Full Load Speed vs. Wave Length. Each curve represents a constant towing force. All wave heights were $a = \lambda/20$.

Figure III - Full Load Dynamic Bending Moment vs. Wave Length for section 1 (forward). Each curve is for a constant towing force. Curves are labeled by still water speeds for the constant towing forces. The inner scale is corrected for still water bending moment.

Figure IV - Full Load Dynamic Bending Moment vs. Wave Length for section 2 (amidships). Same as Figure III except that it is for section 2.

Figure V - Full Load Dynamic Bending Moment vs. Wave Length for section 3 (aft). Same as Figure III except that it is for section 3.

Figure VI - Dynamic Full Load Bending Moments vs. Towing Force for section 2. Each curve is for a constant wave length.

Figure VII - Total Ballast Bending Moment vs. Model Speed. These curves are the same as Figure I except they are for the ballast condition.

Figure VIII - Ballast Condition Speed vs. Wave Length. Each curve represents a constant towing force. All wave heights were $a=\lambda/20$.

Figures IX, X, and XI - Ballast Condition Dynamic Bending Moment vs. Wave Length. These curves are similar to those shown in Figures III, IV, and V respectively, but are for the ballast condition.

Figure XII - Dynamic Ballast Bending Moment vs. Towing Force for section 2. Each curve is for a constant wave length.

Figure XIII - Profile Sketches of the Model in Full Load Condition. The wave condition was $\lambda=L$ and $a=\lambda/20$; the model speed was 0.72 knots. The bow and stern are shown at maximum pitch angles and the long profile shows the model at maximum sagging condition.

Figure XIV - Profile Sketches of the Model in the Ballast Condition. The wave condition was $\lambda=L$ and $a=\lambda/20$; the model speed was 0.59 knots. Bow and stern are shown at maximum pitch angles and the long profile shows the model at zero dynamic bending moment. The model is going from sagging to hogging at this time.

Dynamic bending moments refer to the moments measured in the tests. Still water calculated moments are those computed from the ship data. The left outside scale on the

curves refers to the dynamic bending moments. The still water bending moments have been drawn across the plots in the proper direction to serve as zero points for the total bending moments on the inside scale.

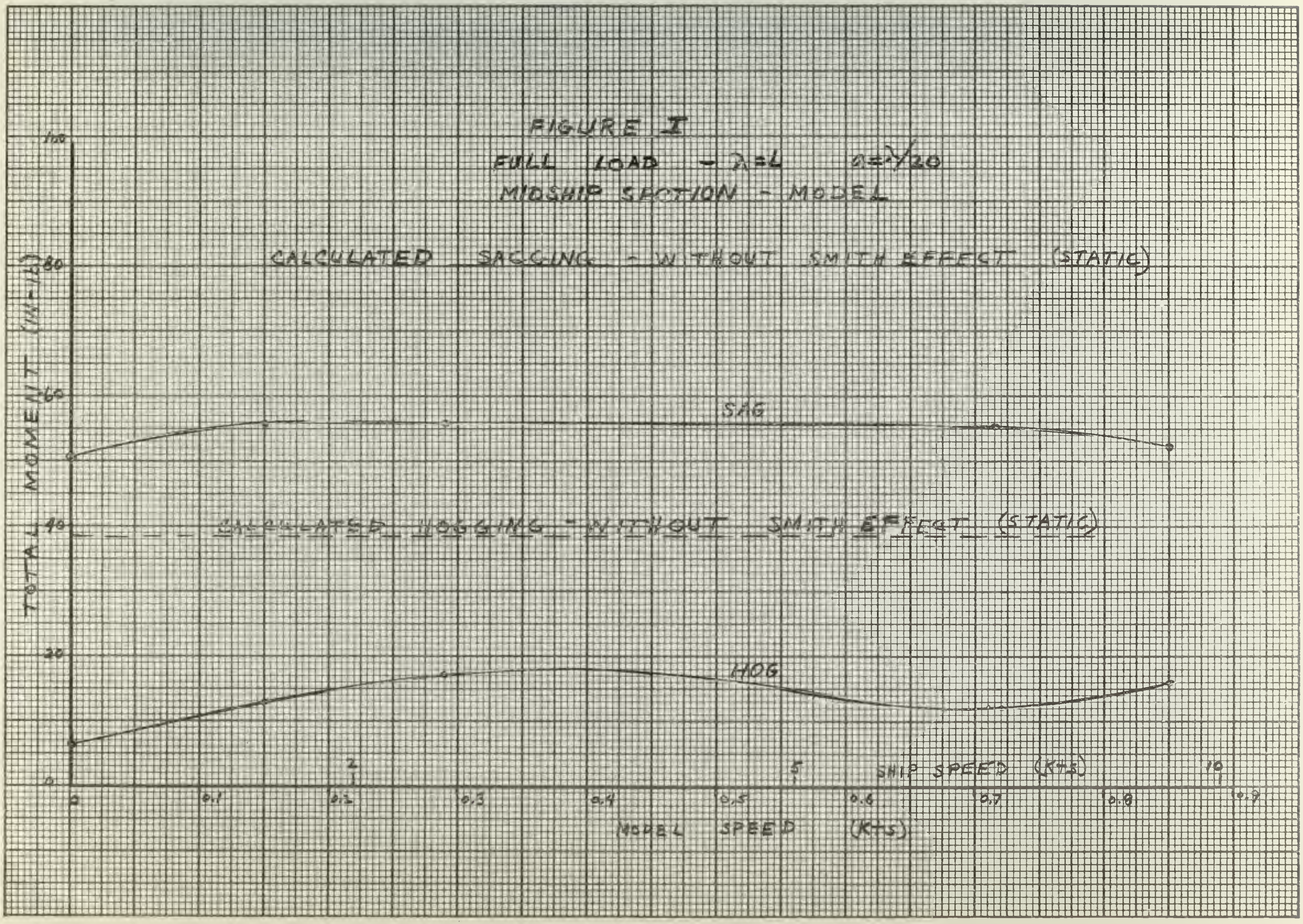
FIGURE I
FULL LOAD - λ=L a=L/20
MIDSHIP SECTION - MODEL
CALCULATED SAGGING - WITHOUT SMITH EFFECT (STATIC)
SAG
CALCULATED HOGGING - WITHOUT SMITH EFFECT (STATIC)
HOG
TOTAL MOMENT (IN-LB)
100
80
60
40
20
0
SHIP SPEED (KTS)
2
5
10
0
0.1
0.2
0.3
0.4
0.5
0.6
0.7
0.8
0.9
MODEL SPEED (KTS)

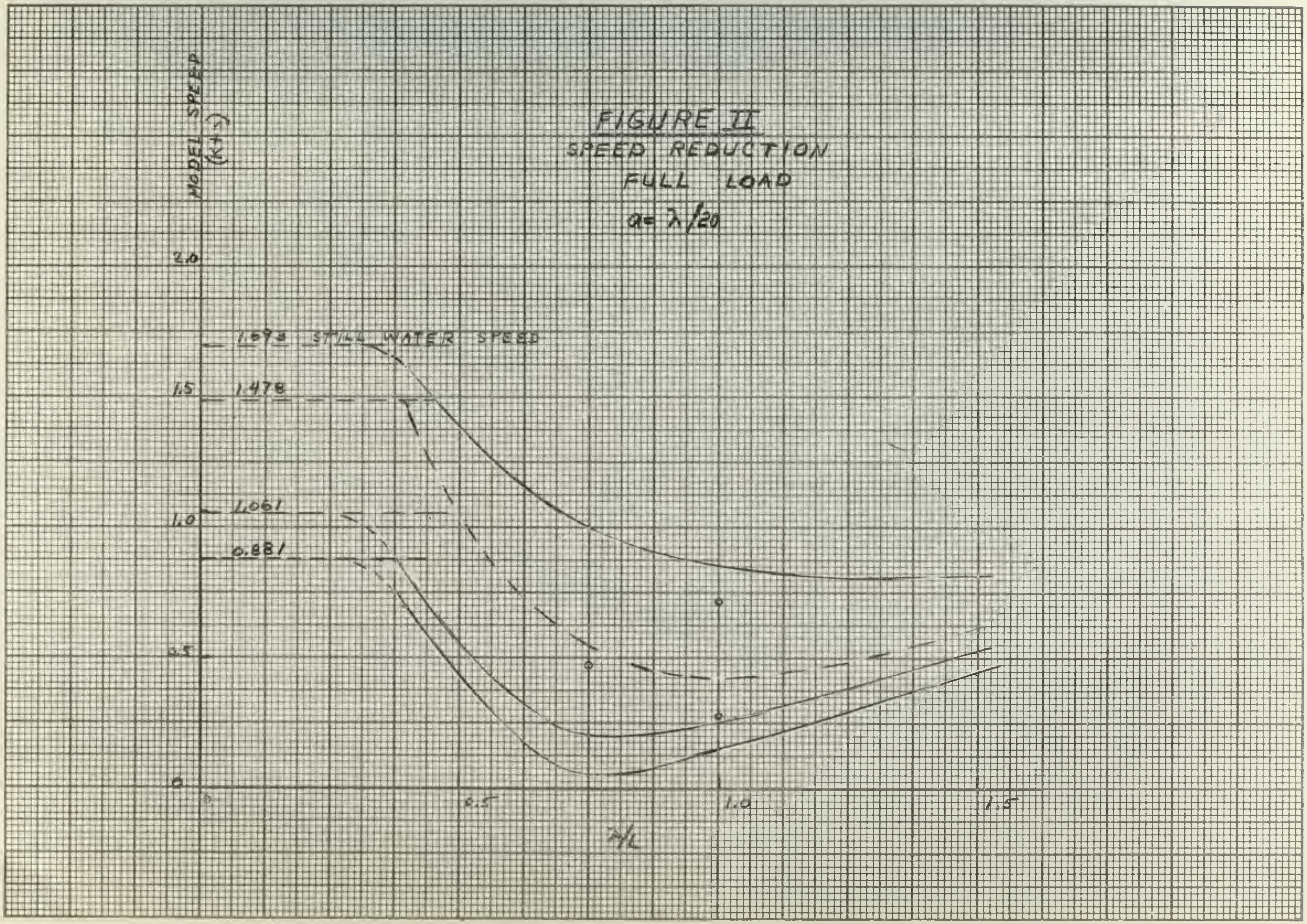

FIGURE II
SPEED REDUCTION
FULL LOAD
$a = \lambda/20$
MODEL SPEED (k+)
2.0
1.5
1.0
0.5
0
1.673 STILL WATER SPEED
1.478
1.061
0.881
0.5
1.0
1.5
λ/L

FIGURE III

FULL LOAD - FORWARD SECTION

$a = \lambda/20$

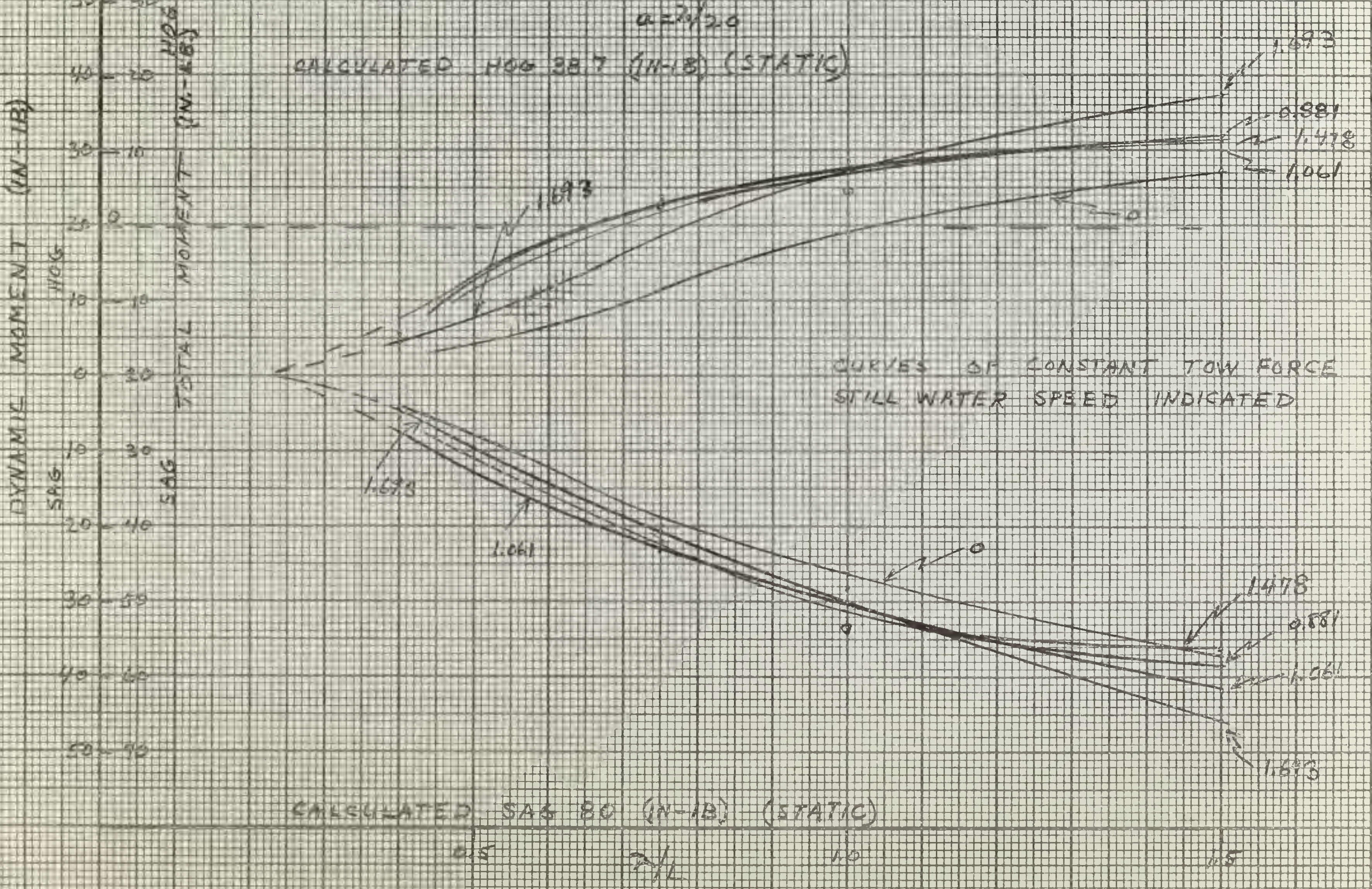

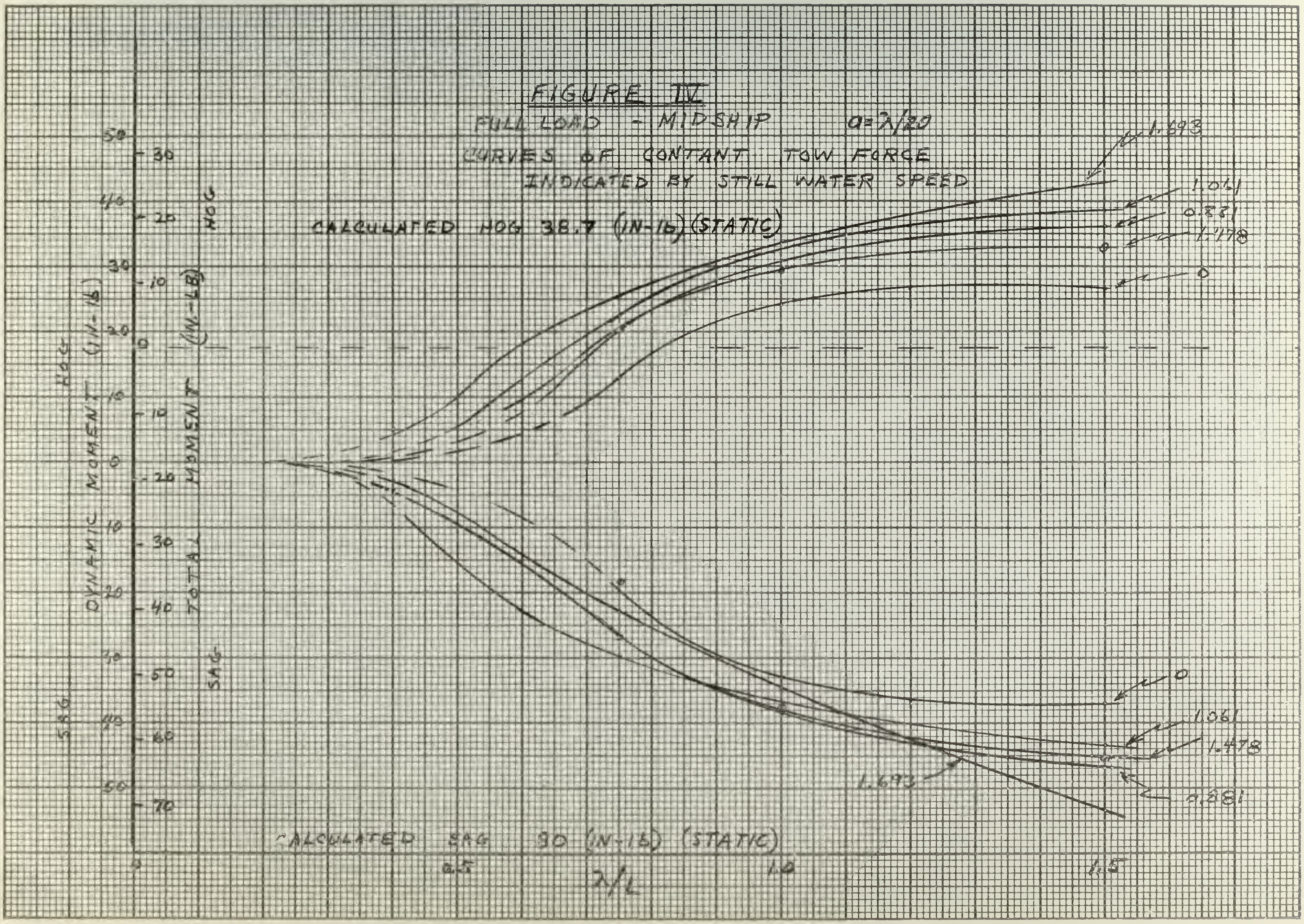

FIGURE IV
FULL LOAD - MIDSHIP a=λ/20
CURVES OF CONTANT TOW FORCE
INDICATED BY STILL WATER SPEED
CALCULATED HOG 38.7 (IN-lb) (STATIC)
CALCULATED SAG 80 (IN-lb) (STATIC)
1.693
1.061
0.881
1.178
0
0
1.061
1.478
0.881
1.693
HOG
DYNAMIC MOMENT (IN-lb)
SAG
TOTAL MOMENT (IN-LB)
HOG
SAG
λ/L
0
0.5
1.0
1.5

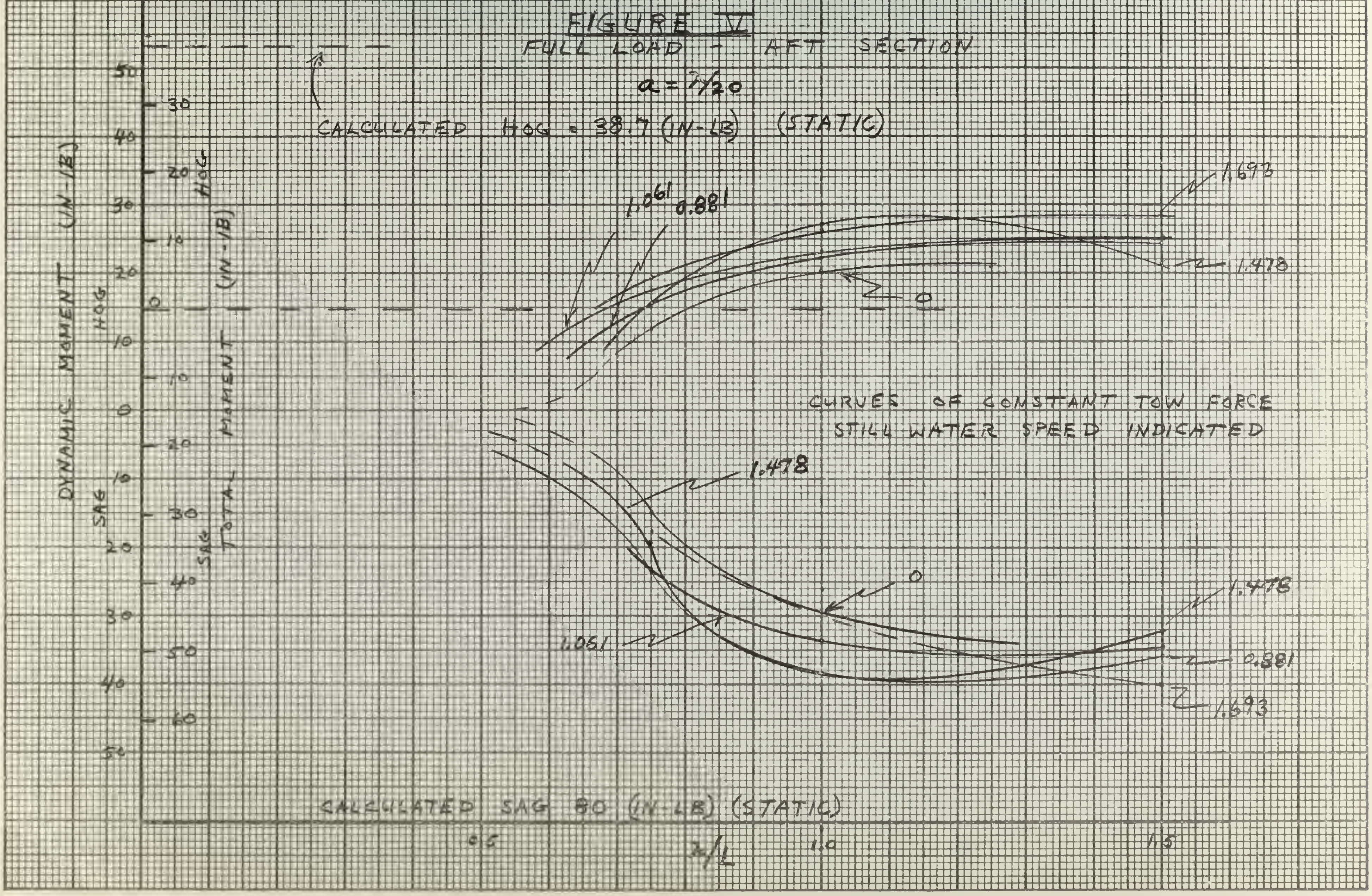

FIGURE V
FULL LOAD - AFT SECTION
$a = \lambda/20$
CALCULATED HOG = 38.7 (IN-LB) (STATIC)
CURVES OF CONSTANT TOW FORCE
STILL WATER SPEED INDICATED
1.693
1.478
1.061
0.881
0
CALCULATED SAG 80 (IN-LB) (STATIC)
DYNAMIC MOMENT (IN-LB)
TOTAL MOMENT (IN-LB)
HOG
SAG
λ/L
0.5
1.0
1.5

FIGURE VI

FULL LOAD - MIDSHIP SECTION

$a = \lambda/20$

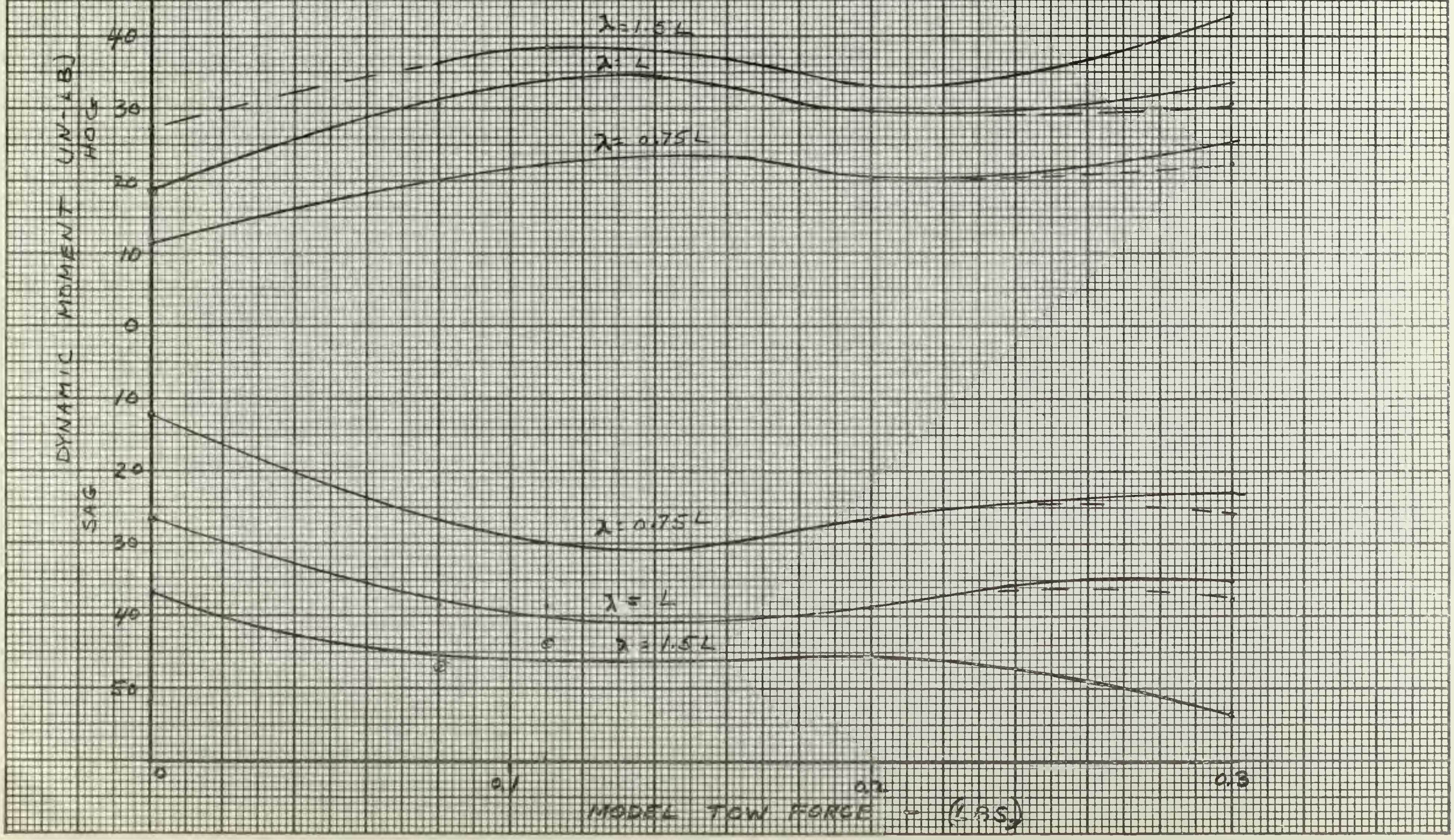

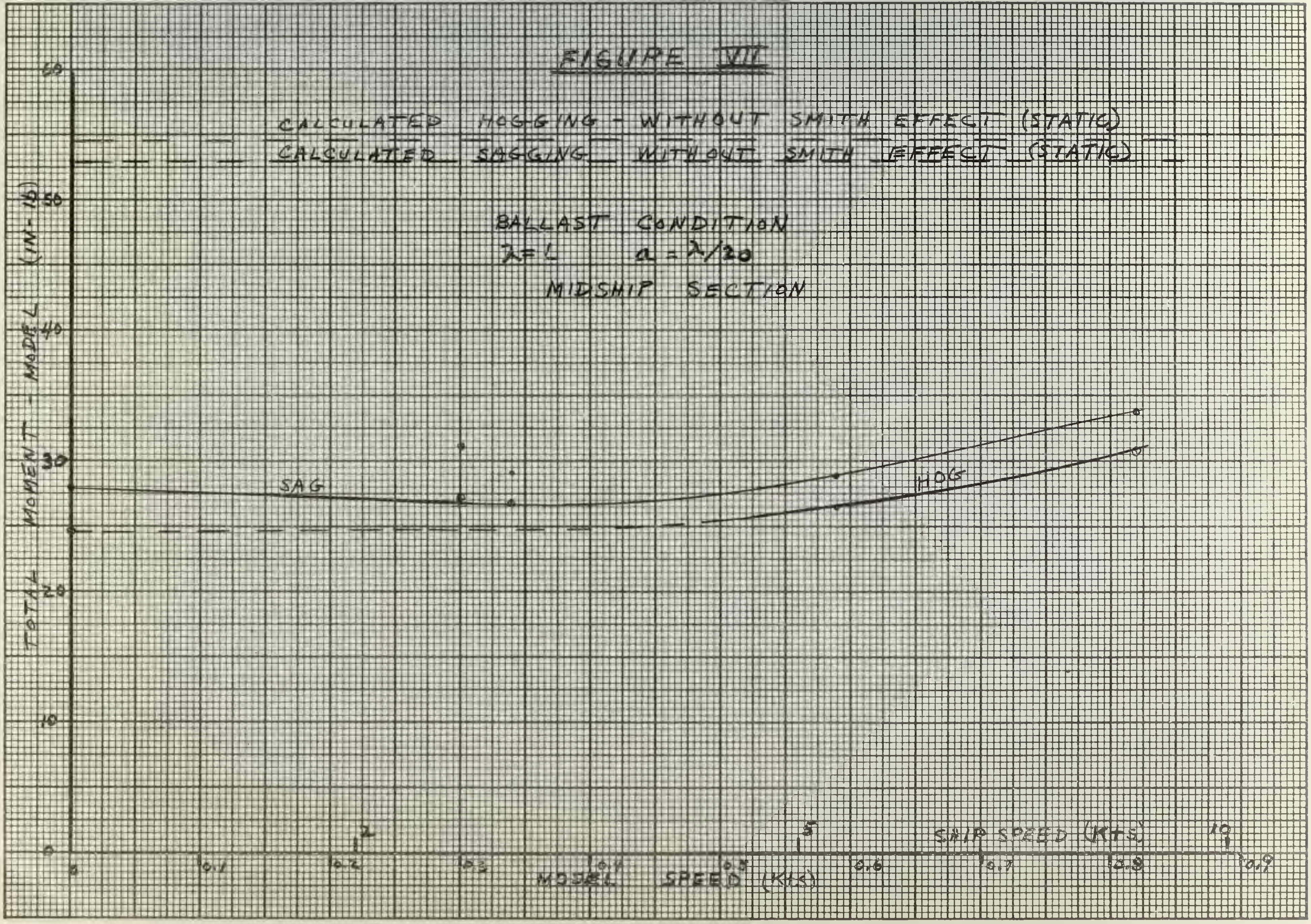
FIGURE VII
CALCULATED HOGGING - WITHOUT SMITH EFFECT (STATIC)
CALCULATED SAGGING WITHOUT SMITH EFFECT (STATIC)
BALLAST CONDITION
λ = L   a = λ/20
MIDSHIP SECTION
SAG
HOG
TOTAL MOMENT - MODEL (IN-LB)
0
10
20
30
40
50
60
MODEL SPEED (KTS)
0.1
0.2
0.3
0.4
0.5
0.6
0.7
0.8
0.9
SHIP SPEED (KTS)
2
5
10

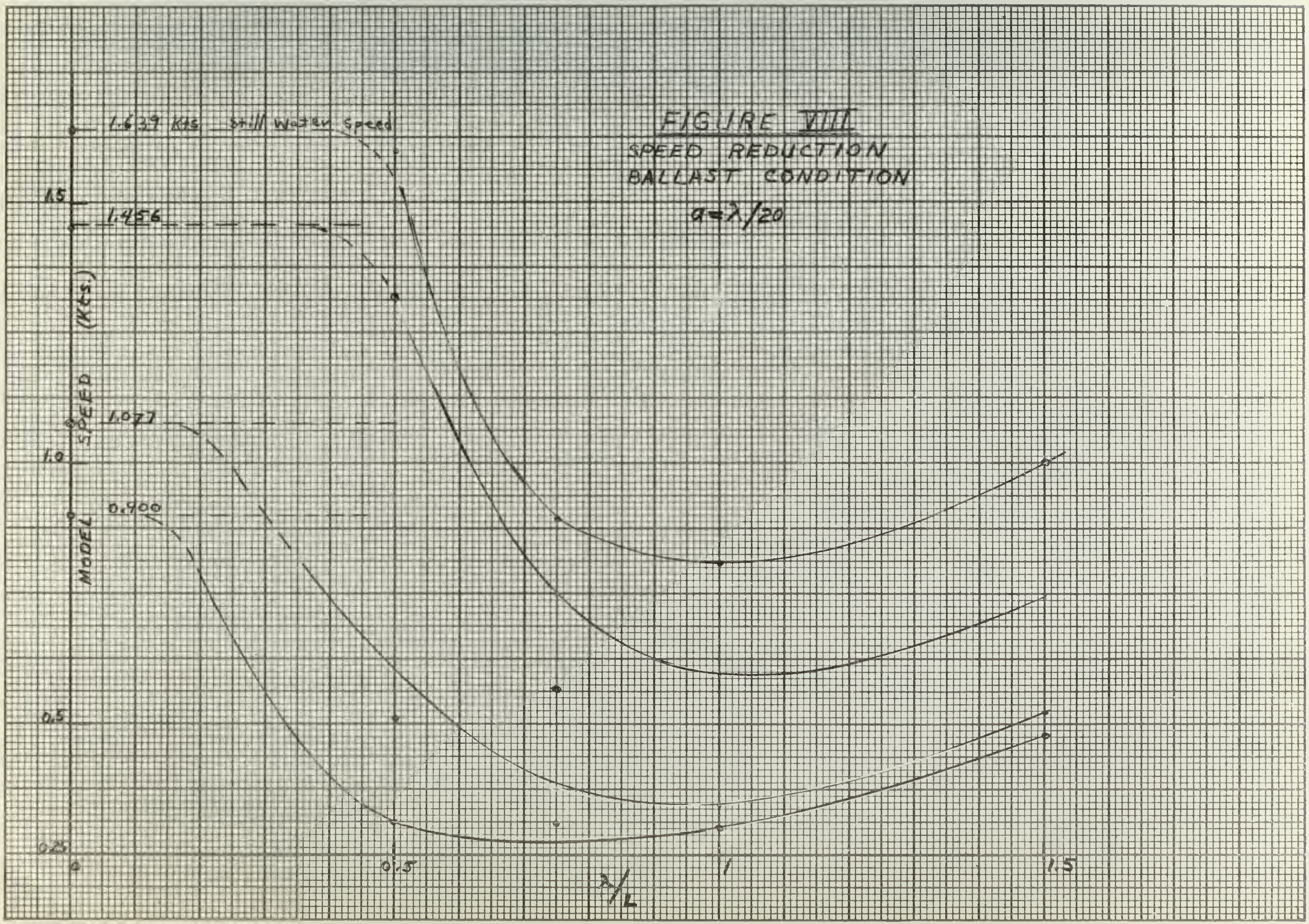

FIGURE VIII
SPEED REDUCTION
BALLAST CONDITION
a=λ/20
1.639 Kts still water speed
1.456
1.077
0.900
MODEL SPEED (Kts.)
1.5
1.0
0.5
0.25
0
0.5
1
1.5
λ/L

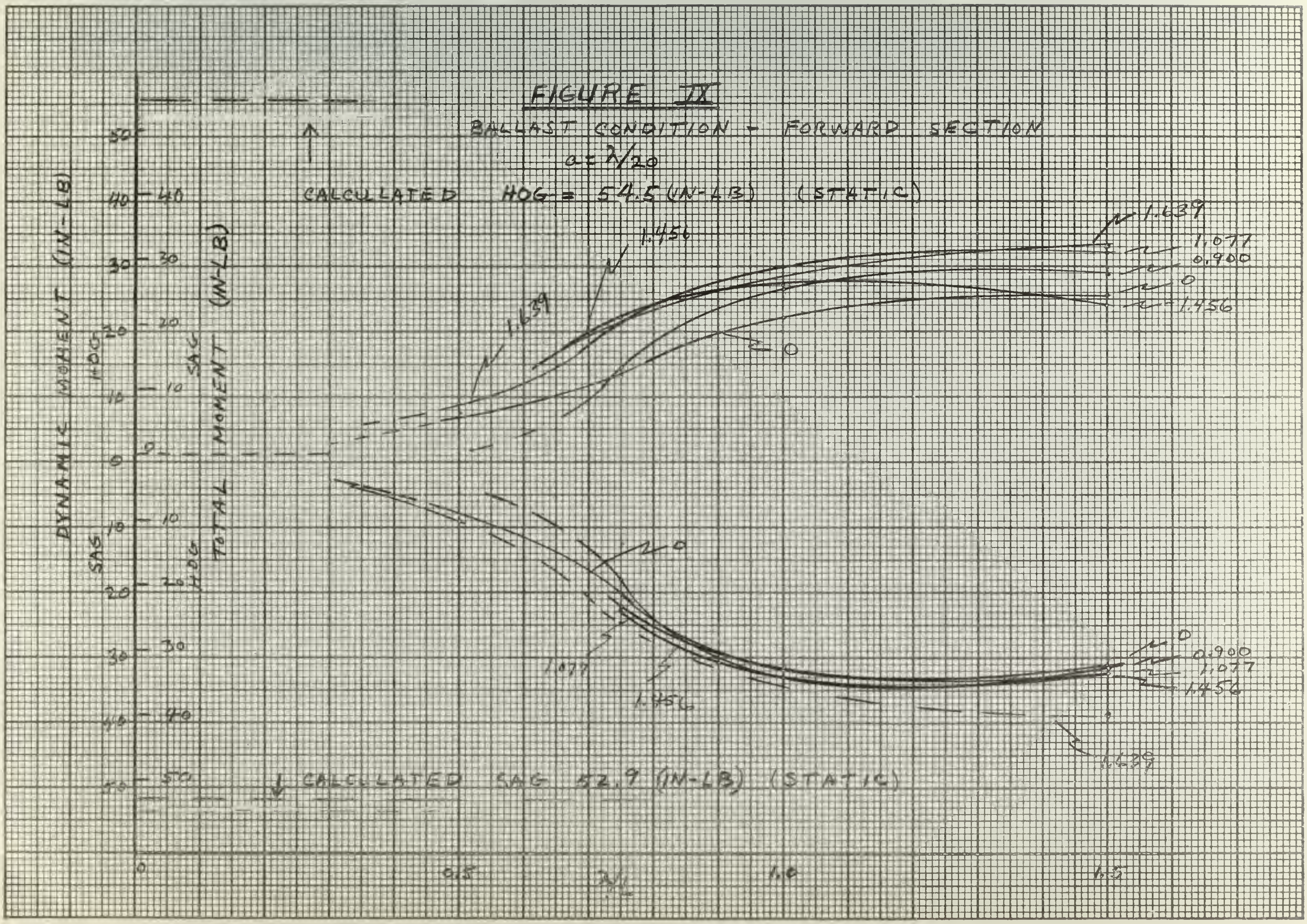
FIGURE IX
BALLAST CONDITION - FORWARD SECTION
a = λ/20
CALCULATED HOG = 54.5 (IN-LB) (STATIC)
CALCULATED SAG 52.9 (IN-LB) (STATIC)
DYNAMIC MOMENT (IN-LB)
TOTAL MOMENT (IN-LB)
HOG
SAG
1.639
1.077
0.900
0
1.456
λ/L
0.5
1.0
1.5

FIGURE X

BALLAST CONDITION - MIDSHIP SECTION

$a = \lambda/20$

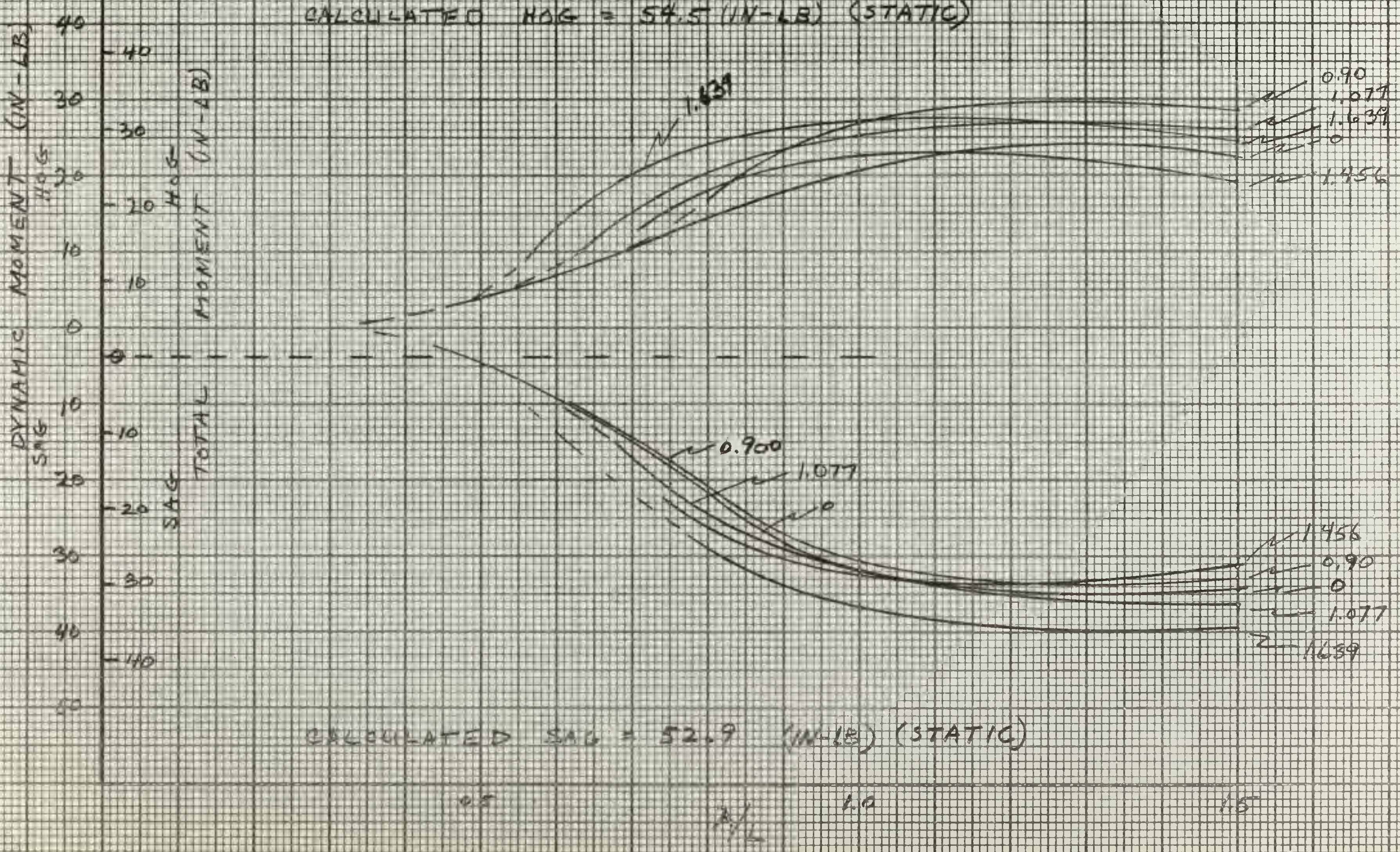

FIGURE XI

BALLAST CONDITION - AFT SECTION

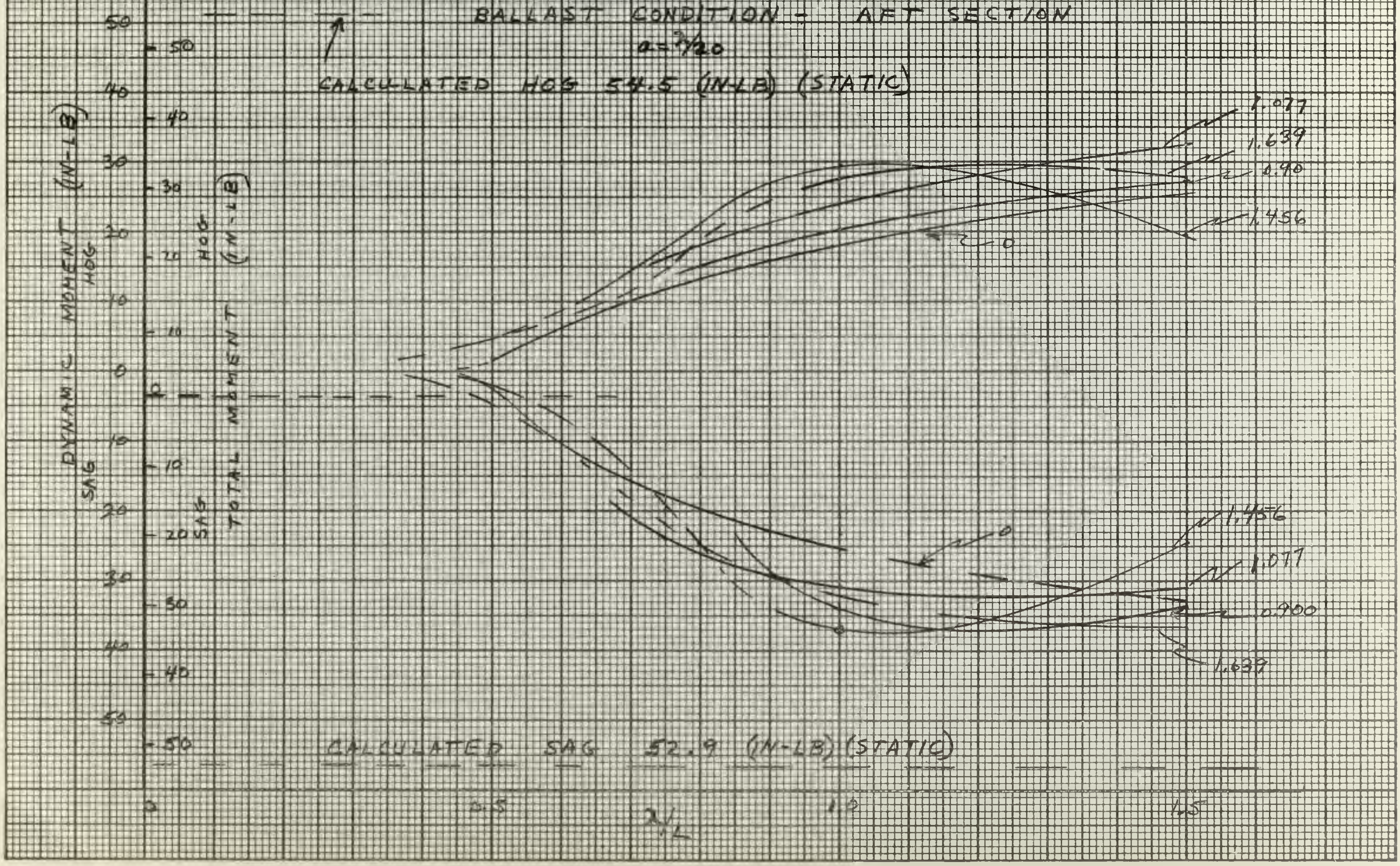

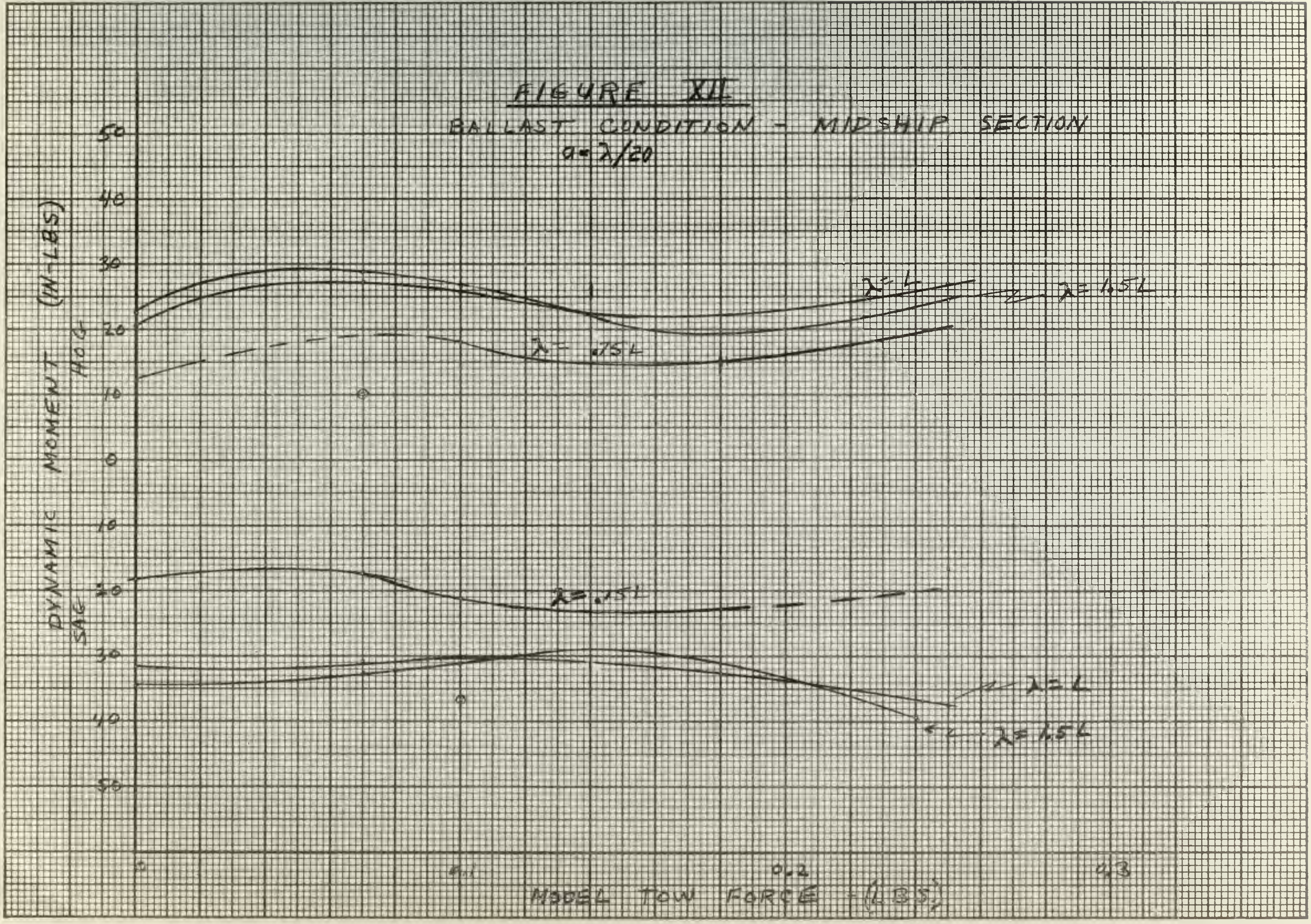

FIGURE XII
BALLAST CONDITION - MIDSHIP SECTION
$a = \lambda/20$

FIGURE XIII

PROFILE IN WAVES - RUN 3

FULL LOAD V_V =0.72 Kts.

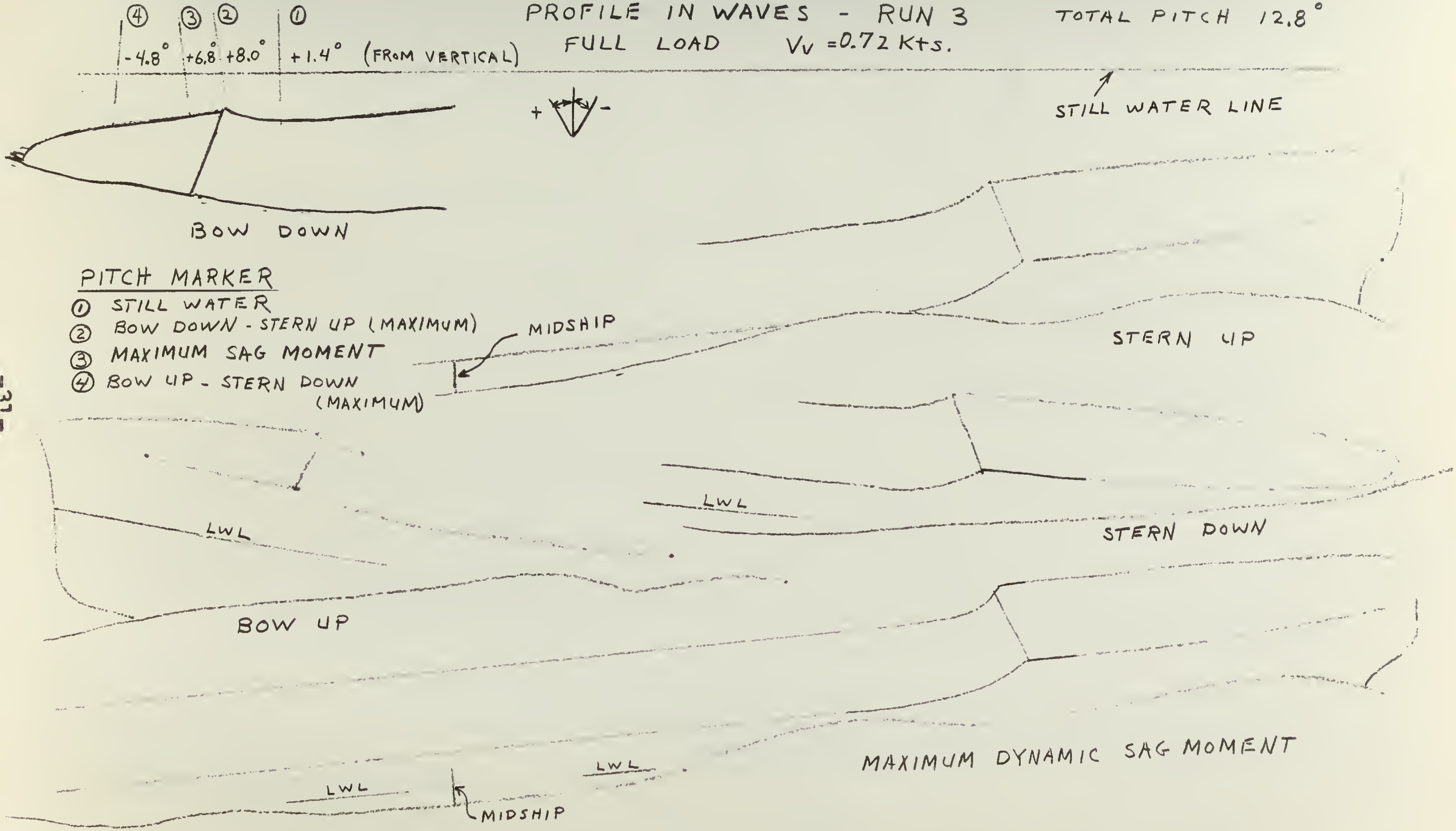

NOTE: PITCH MARKER AT POSITION ① IS A REFERENCE ONLY

FIGURE XIV

PROFILE IN WAVES - RUN 48
BALLAST LOAD V_v = 0.59 Kts

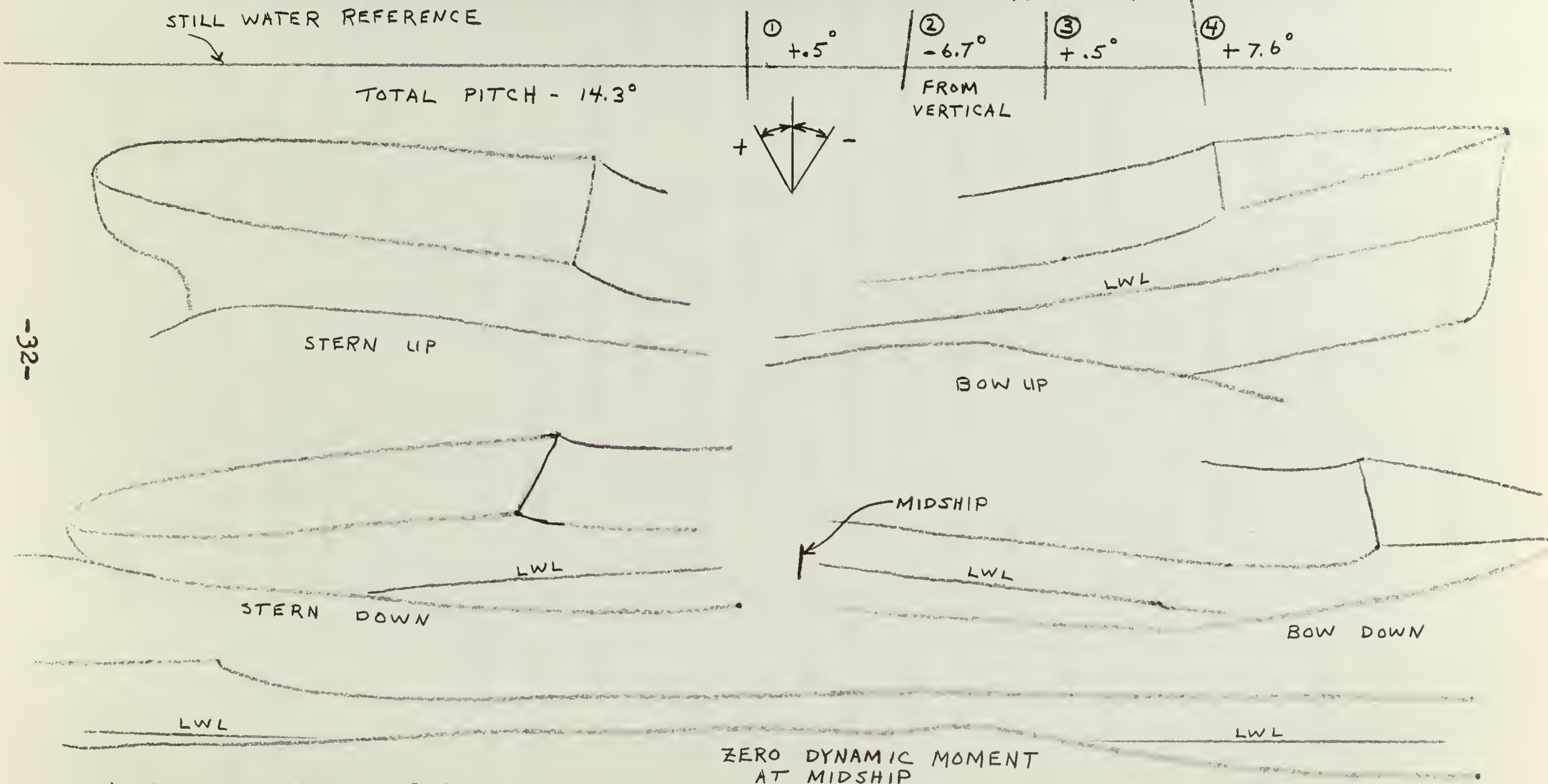

NOTE: PITCH BAR MARKER ①
IS A REFERENCE MARK
OF ITS INITIAL POSITION

PITCH MARKER

① STILL WATER
② BOW DOWN - STERN UP
③ ZERO DYNAMIC MOMENT
④ BOW UP - STERN DOWN

IV. DISCUSSION OF RESULTS

It is important in comparing the model bending test to actual ship conditions to define the bending moments as measured. Due to difficulties in obtaining an absolute zero bending moment in the model (no measurable strain in the flexure bar) only dynamic moments in hogging and sagging, with the still water bending moment considered as zero, were obtained. In the curves these moments were corrected by adding the calculated still water bending moments. These moments were calculated by integrating the weight and buoyancy of the ship in the full load and ballast conditions. These results were then scaled to the model giving the still water moments at sections 1, 2, and 3 (forward, midship, and aft). These individual moments are given in Appendix A. In the full load condition the still water moment increases the sagging moments considerably. For the midship section (Figure IV) the sagging moment increased from its maximum of 53.6 in.-lb. at $\lambda = 1.5L$ to 71.0 in.-lb. This brought the moments in the sagging direction considerably closer to the calculated sagging moment of 80.0 in.-lb. Conversely it reduced the maximum recorded dynamic hogging moment from 43.0 in.-lb. to 25.6 in.-lb. The calculated moment in hogging for the standard wave was 38.7 in.-lb. Therefore the maximum sagging was 89% and the hogging was 66% of the static calculated moments. In both cases these are well within the static calculation.

In the final determination of stresses in the ship other

forces are acting which are not taken into account by our type of instrumentation. Hydrostatic forces are of course acting on the underbody. Compressive forces also exist when the body is moving through the water. In general the effect of compressive forces on bending will be small. Since the flexure bar was at about one-half of the draft from the baseline where the compressive force could be assumed to act, little of the bending effect of this force was transmitted to the flexure bar. However, if in the extreme case we consider a flexure bar at the water line with a draft of 3 inches and the total towing force of .5 lbs. acting horizontally at the bottom of the model (this is greater than the towing forces used) a moment of 1.5 in.-lbs. is applied to the bar. This is of the order of 3% of the maximum moments recorded. Since it was impossible to put the flexure bar on the bottom of model and impractical to fasten it at the main deck level, this effect was ignored. Consequently the bending moment defined is due to the vertical forces.

The calculated bending moments to which the results are compared are those as computed by the owners for the full load and ballast condition as set up by them. They did not include the "Smith Effect" which would reduce the values. The calculated bending moments do not necessarily represent an actual static computation in the standard wave. The method used by the owner consisted of calculating the bending moments for four drafts and four trim conditions in the hogging and sagging condition. This was done for all three sections, 1, 2 and 3

(96 computations). Any condition of loading could then be interpolated from these data. Whether the full load and ballast conditions used were obtained by interpolation or actual computation is not known. It is felt that this method is acceptable and any error would be small.

The experiment was performed throughout on the basis of constant towing forces after having established the still water speeds for each force. The speed reduction curves are Figures II and VIII. These are consistent with results as predicted by Professor M. A. Abkowitz's paper, Reference (1). As pointed out in this paper the constant towing force method of towing is practically equivalent to the ship condition of maintained E.H.P. or maintained R.P.M. This is most desirable for comparison purposes. Both the full load and ballast condition speed reduction curves show greatest speed reduction at wave lengths of 0.75L. With the equipment used in the M.I.T. Towing Tank (see Reference (2)) surge, pitch, and heave are unrestrained and some amount of rolling is possible.

Figure I gives the bending moments for full load over the speed range which may be expected in normal operation of the ship in a wave condition of $\lambda = L$ and $a = \lambda/20$. No radical change was recorded from 1 to 10 knots ship speed. These results seem to agree with those obtained by Mr. E. V. Lewis in Reference (8) with a T-2 tanker in the operating speed range. A slight trend is shown at the highest speed towards reduced bending moments in sagging and increased moments in hogging. Resonance between pitch period and encounter period

is reached at 1.3 kts model speed at $\lambda = L$. At a first glance it might seem that lower bending moments should be observed as the model reaches resonant speed for any given wave length. Figure VII giving the bending moments for the ballast condition shows the opposite trend of increasing bending moments as the model approaches resonant speed. In this case T_p is almost the same as for full load. Unfortunately the heaving periods of the model were not observed. Perhaps the coupled effects of both pitch and heave could be related with some consistency to the data.

There is still the speculation as to whether the maximum pitching amplitudes occur when the period of wave encounter is equal to the still water period of pitch. This refers also to the heave. Dynamic exciting forces could act in such a way as to produce greatest pitching amplitudes away from the point where $T_p/T_e = 1$. It is felt that some correlation exists between pitching, heaving, surging, and the bending moments. Since only the bending moments were observed and not these related characteristics no formal attempt for correlation is justified at this stage.

In Figures III, IV and V the bending moments were plotted against λ/L. The curves are labeled by still water speeds which in turn represent constant towing forces. The equivalent towing forces may be found in Table I . This was done so that the reader could visualize the magnitude of the still water speed. The bending moments for each section were plotted separately since the still water bending moment for each

section varied slightly. All three groups of curves retain the same general character and within the limits of experimental accuracy apparently duplicate each other. The main purpose of measuring the bending moments at three sections was to see if indeed the midship section will give the greatest bending. The midship section definitely has the largest range from sagging to hogging. The values for the range were 97 inch-pounds for section 2 (amidship), 83 inch-pounds for section 1 (forward) and 69 inch-pounds for section 3 (aft). Though sections 1 and 3 were evenly spaced from amidships, there is a difference of 15 inch-pounds in their bending moment ranges or a variation of 15.5% of the maximum range (midship section).

Besides the range between hogging and sagging being larger at amidships, the moments in both hogging and sagging are slightly larger at $\lambda = 1.5L$. Section 2 has a total hogging moment at 0.82 knots (1.693 still water speed) 8.1 inch-pounds greater than section 1 and 12.3 inch-pounds greater than in section 3. Similarly for the sagging condition section 2 is 5.4 inch-pounds and 15.8 inch-pounds greater than sections 1 and 3 respectively. Inspection of the curves discloses that the highest towing forces do not necessarily produce the highest bending moments at all wave lengths. At $\lambda = L$ all the towing forces (except zero) give larger bending moments. At $\lambda = 1.5L$ we have the interesting phenomena of having the maximum bending moments at 1.693 knots still water speed and minimum at 1.478 knots. At the two towing forces smaller than

either of these the moments lie between these points. The same results pertain to all three sections which were recorded independently.

According to the speed reduction curve the speed in waves decreases in the same order as the towing forces, i.e., the highest towing force also has the highest speed for each wave length. As mentioned previously the synchronous speed for pitching is greater than those encountered at this wave length ($\lambda = 1.5L$). If speeds nearest the synchronous speed produced lowest bending moments this would mean that the bending moments should be in the same order as the speeds which isn't true in this case. It is therefore suspected that the vertical accelerations of heave have an influence on the bending moments, and may be the cause for the inversion. In any case for all the towing forces the moments seem to have reached their peak values at $\lambda = 1.5L$. More investigation at greater wave lengths is necessary to confirm this.

Dynamic bending moments below $\lambda = 0.5L$ are negligible in magnitude. They are roughly proportional to λ between $\lambda = 0$ and $\lambda = L$. Professor E. V. Lewis in Reference (8) shows a similar proportionality for bending moments vs. wave heights at constant wave length. Considering the still water bending moment one can see that the hogging condition is not attained before the range of $\lambda = 0.6L$ to $0.85L$ depending on the speed. At zero speed the model did not have a corrected hogging bending moment until $\lambda = 0.85L$. The greater the towing force, the lower the wave length was, in the range given, to produce a

hogging moment. Below $\lambda = 0.4L$ dynamic moments are less than 5 in.-lbs. and could not be recorded due to excessive vibration on the low attenuator scales on the recording equipment.

In the speed or towing force range investigated, Figures III, IV, and V actually show little variation of bending moment at one wave length. Considering section 2 the greatest variation occurs at $\lambda = 1.5L$. This is only about 15% of the total range (hogging and sagging).

Figure VI is a plot of the dynamic moments against towing force. This plot gives additional information over Figure I in that $\lambda = 0.75L$, and $\lambda = 1.5L$ are included. The change of abscissa from speed to towing force magnifies the differences. The hogging moments follow a general trend and suggest dependence on the towing force rather than actual speed, as the humps and hollows occur at the same towing forces for all wave lengths. Unfortunately the sagging moments show a less clearly defined trend. Here again a greater range of towing forces would be valuable in determining the curve more accurately. It is possible that the zero error has increased the hogging moments and decreased the sagging moments at the highest towing force. Assuming that this is true we have increased the sagging moments and decreased the hogging moments 3 to 5 inch-pounds for runs No. 4 and No. 9. Thus all the moments show the same trends, have just gone through a hollow at 0.20 lbs. towing force, and will increase in magnitude at greater towing force. The $\lambda = 1.5L$ curve shows this characteristic best.

Figure VII is the first curve for the ballast condition

and can be compared with Figure I for full load. This ballast condition is only one of several offered by the ship owner for investigation. The bending moments corrected for still water bending moment are plotted for $\lambda = L$ and $a = \lambda/20$. Here again speeds considered in the operating range were investigated. Due to slamming which was quite noticeable in the motion picture films taken, 10 knots might well be considered the maximum speed allowable for this type ship in such waves. The still water bending moments (Appendix A) were quite small and varied from 1.2 inch-pounds sagging in section 1 to 3.8 inch-pounds hogging in section 2. The curves indicate that the bending moments will increase with speed in waves for the range investigated. The total hogging moments at comparable speeds are slightly higher in the ballast condition than in the full load condition, while the total sagging moments are lower than for the full load. This is due largely to the difference in still water moments between the two conditions. The static calculations have changed their relative positions, being slightly greater in hogging than in sagging. The maximum total sagging moment at section 2 is 68% of the calculated static moment and the maximum hogging is only 61%. Assuming that the ship was designed for the full load calculated bending moments the ballast condition maximum moments would have been 45% of the static calculation in sagging, and 86% in hogging. The full load condition is the controlling condition in this case. However, it is felt that more critical ballast loadings were available for investigation and should be tested

before assuming that the ballast condition is safer than full load.

Figure VIII which is the speed reduction curve needs no explanation. It is noticed that the greater reduction of speed occurs in the full load condition rather than in ballast which seems logical considering the difference in draft.

Figures IX, X and XI for the ballast condition are similar in form to Figures III, IV, and V for the full load tests on similar coordinates. The results obtained however were more scattered and the trends are not all consistent. Considerable trouble was experienced with the recording equipment in determining the zero for the dynamic bending moments. Therefore it is felt that the range (hog plus sag) for these runs were more accurate than the individual sagging or hogging moments recorded. Examination of the recorder tapes indicate that zero errors of the order of 4 to 6 in.-lb. are possible. Apparently in the light load condition minor movements of the strain gage wiring (held by a fish pole rig) were enough to change the zero reading.

Ignoring some apparently poor points the envelope of the curves for the three sections indicate that the range of bending moments for all three sections is just about the same. The dynamic moments of section 2 are slightly larger in the order of magnitude of 2 to 3 in.-lbs. This is in contrast to the full load condition where midship section was in the order of 15 in.-lbs. larger than the other two sections. The range between hogging and sagging is the greatest at $\lambda = 1.25L$

and is equal to 70 in.-lb. This again is considerably smaller than the 97 in.-lb. range for the full load at the midship section.

The still water bending moments for the ballast condition are of small magnitude as mentioned previously. This moves the wave length at which the ship will have sagging moments from the 0.6L to 0.85L range discussed for full load to a range of 0.25L to 0.5L for the ballast condition. Thus the ship will develop sagging moments considerably sooner in the ballast condition as the wave length is increased (at constant wave slope) than hogging moments were developed in full load.

If the curves are relocated by small shifts, conceivably due to zero error (sections 2 and 3), the same tendency is observed as in full load. At λ=1.5L the bending moments at the highest speed are greatest while the next lowest speed drops considerably. Runs with lower towing forces range between these values. This trend is exactly that noticed in Figures III, IV, and V. Further investigation at points in this range is needed to confirm this trend. The forward section data was not as reliable as that for the other sections, as some trouble was encountered with the strain gages at this location or the recorders during the latter part of the experiment.

Figure XII plots the bending moment against towing force for section 2. Here again the same type of hump exists in the hogging moments, though in this case the curves cross each other whereas they did not in the similar plot for full load.

The sagging moments show a remarkable tendency to remain of the same magnitude for towing forces of .07 to .17 lbs. The moments beyond this point increase. Points beyond .25 lbs. towing force should be investigated further since Figures IX, X, and XI indicate that the bending moment at this towing force has just about reached its maximum.

Figure XIII is the sketch of the model at full load in a $\lambda = L$ wave at 0.72 knots (1.478 knots still water speed.) The sketches were made from the motion picture films by tracing the projection of them on a screen. The bow and stern are shown at maximum pitch angles of 6.6 degrees down by the bow and 6.2 degrees down by the stern. The horizontal lines are the still water reference lines and the lines in the vertical direction show the angles made by the pitch bar affixed to the model. The model's forefoot emerged slightly when the bow came up, and only a small amount of "digging in" as observed when the bow went down. The sketch at the bottom of the Figure shows the position of the model when the electric eye made a marker on the recording tape. At this point the dynamic bending moment was at a maximum sagging value at section 2 of 33 inch-pounds. This is 5 inch-pounds less than the average of the highest sagging moments recorded for this wave condition. Corrected for still water moment the total sagging moment was 50.4 inch-pounds (amidship).

Figure XIV presents sketches of the model in ballast loading in a $\lambda = L$ wave with $a = \lambda/20$. A considerable portion of the bow emerged when it rose in pitching, but the model

did not "dig in" when the bow dropped. Maximum stern immersion did not occur at maximum pitch angle. The maximum pitch angles for the ballast condition were 7.2 degrees down by the bow and 7.1 degrees down by the stern. The long profile is a sketch of the model at zero dynamic bending moment or 4 inch-pounds total bending moment (amidships).

Accuracy of the Results

The magnitude of individual errors in the loading of the model, instrumentation, and data is difficult to ascertain without attempting to duplicate the loadings and tests again. This would be one way to see how closely the data could be reproduced.

The scales used to weigh the model and the individual weights had an accuracy of plus or minus 0.02 pounds. It must be remembered that this accuracy is not obtained on the total model weight, but on the individual components of ballast, towing bracket, etc. The total weight error of about 1% was small compared with the error involved in assuming the full load or ballast condition. The ship data, as obtained from the weight curve, capacity plan, and strength tables contained conflicting information of the order of 3% for any chosen load. Since a 34.4% difference between the displacements in full load and ballast conditions affected the bending moment of the model by approximately 25 inch-pounds (total range), 3% error in loading would cause a possible error of 2.2 inch-pounds. This is only 2.2% of the

total full load condition range of bending moments.

The instrumentation (Sanborn Recorders) has an accuracy of within 2%. This again is quite small. The greatest difficulty in obtaining accurate results was establishing the zero reference point of the still water condition for dynamic bending moments. Moving the "fish pole" while setting this zero on the recorders was observed to cause deflections of 4 to 6 inch-pounds. Errors up to 10% were therefore possible in establishing the zero reference. However, this does not affect the accuracy of the range (hogging plus sagging) of the dynamic moments. As the results indicate, the zero error was consistently well under 10%.

There was also a possible error in the bending moments due to variations in the wave heights. Variations of 1/4 inch in 3 inch wave heights were observed in one run. This is an error of plus or minus 4% and indicates an error of plus or minus 4% in the bending moment, assuming that the bending moment is proportional to the wave height at constant wave length. Only the maximum bending moments were averaged so this leaves a possibility that the bending moments reported may be 4% high.

Summing up these errors, but keeping in mind the general consistency of our results, it appears that the overall accuracy of our results is about 10%, certainly not more than 15% on individual points except for an occasional erratic point.

V. CONCLUSIONS

From the foregoing discussion it is concluded that:

1) The measured longitudinal bending moments for the model were well below the values obtained by the static design calculation.

2) For a given wave length and height, speed variation within the operating range of the ship has small effect on the longitudinal bending moments.

3) Our results compare well with the results obtained in previous tests in general trends, in particular the results of Professor E. V. Lewis described in Reference (8) as concerns conclusions 1) and 2) above.

4) Dynamic bending moments are negligible up to a wave length of about 0.25L. The increase is then rapid and approximately linear until a wave length equal to the ship length is reached.

5) For this ship the bending moment appears to peak at a wave length equal to 1.5L.

6) The bending moments at the midship section were the greatest, both in ballast and full load conditions.

7) The bending moments in the ballast condition investigated were less than those obtained in the full load condition.

VI. RECOMMENDATIONS

1. Speeds somewhat greater than the operating range should be investigated to assure the trend of the curves plotted in this thesis.
2. A model to be cut should be well varnished or painted inside and out to waterproof it and completely seal the wood. This is necessary to prevent water from separating the lifts.
3. A carriage over the model to carry electrical leads to the model should be used to prevent false zero readings in future tests.
4. Maximum output from the strain gages is necessary due to the small strains encountered in this type of testing; therefore, gages of the highest sensitivity should be used.
5. Since the Sanborn Recorder tapes measure only 25 millimeters wide from the middle or "zero" to the full scale reading, when used as in this thesis, and it is possible to read to about one-half millimeter, there is an inherent error of plus or minus 2%. This is increased of course when the records being measured do not use the full width of the tape. It is therefore recommended that other equipment having much wider records, to give larger and more accurate readings, be used in such tests.
6. Other ballast conditions of the ship should be investigated to determine the ballast conditions with the greatest and the least bending moments.

VII. BIBLIOGRAPHY

1. Abkowitz, M. A., "Seakeeping Considerations in Design and Research", paper presented to the New England Section SNAME*, January, 1957.

2. Abkowitz, M. A., and Paulling, Jr., J. R., "The Ship Model Towing Tank at M.I.T.", Trans. SNAME, vol. 61, 1953, pp. 65 - 97.

3. Akita, Y. and Ochi, K., "Model Experiment on the Strength of Ships Moving in Waves", Trans. SNAME, vol. 63, 1955, pp. 203 - 236.

4. Arnott, D., "Strength of Ships", Chapter VI of "Principles of Naval Architecture", vol. 1, edited by H. E. Rossell & L. B. Chapman, SNAME, New York, N.Y., 1941.

5. Bull, F. B., and Baker, J. F., "The Measurement and Recording of Forces Acting on a Ship at Sea", Trans. I.N.A., vol. 91, London, 1949, p. 29.

6. Jasper, N. H., "Study of the Strain and Motions of the USCGC Casco at Sea", DTMB Report 781, 1953

7. Korvin-Kroukovsky, B. V., "Investigation of Ship Motions in Regular Waves", Trans. SNAME, vol. 63, 1955, pp. 386 - 435.

8. Lewis, E. V., "Ship Model Tests to Determine Bending Moments in Waves", Trans. SNAME, vol. 62, 1954, pp. 426 - 490.

9. Lewis, E. V., "Ship Speeds in Irregular Seas", Trans. SNAME, vol. 63, 1955, pp. 134 - 202.

10. Lewis, F. M., "The Inertia of Water Surrounding a Vibrating Ship", Trans. SNAME, vol. 37, 1929, p. 1.

11. St. Denis, M. S., and Pierson, Jr., W. J., "On the Motions of Ships in Confused Seas", Trans. SNAME, vol. 63, 1953, pp. 280 - 357.

12. Taylor, J. L., "Dynamic Longitudinal Strength of Ships", Trans. I.N.A., vol. 88, London, 1946, p. 328.

13. Wachnik, Z. G., and Robinson, D. P., "A Study of Bending Moments in a Ship Model Moving in Waves", B. S. Thesis, M.I.T., May, 1956.

* Society of Naval Architects and Marine Engineers

VIII. APPENDIX

APPENDIX A

Summary of Data and Calculations

1. Model and Ship Principal Dimensions:

   a. Type - Tanker

   b. Scale Ratio 126

	Model	Ship
c. Displacement (full load)	45.60 lbs.	41,785 tons (U.S.)
d. Displacement (ballast)	30.00 lbs.	27,450 tons (U.S.)
e. Design Speed (service)	1.47 kts.	16.5 kts.
f. Length	5.00'	630.0 ft.
g. Beam	0.706 ft.	89.01 ft.
h. Draft - Full load	3.23 in.	33.85 ft.
i. Draft - Ballast	2.19 in.	23.00 ft.
j. Block Coef.	0.776	0.776

2. Computed Model and Ship Characteristics:

   a. Two-Noded Vertical Frequency of Vibration

	Model	Ship
Full Load	9.76 c.p.s.	0.870 c.p.s.
Ballast	10.7 c.p.s.	0.952 c.p.s.

   b. Water Inertia Effect 13.3 lb./ft.

   c. Still Water Bending Moments

		Model	Ship
Full Load:	Forward (Sag)	19.8 in.-lb.	58,797 ton-meters
	Midship "	17.4 in.-lb.	51,673 "
	Aft "	14.85 in.-lb.	44,140 "

Ballast: Forward (sag)	1.16 in.-lb.	3,442	ton-meters
Midship (hog)	3.82 in.-lb.	11,380	"
Aft "	3.64 in.-lb.	10,811	"

d. Design Bending Moments as calculated by Ship Owner on Standard wave - excluding Smith Effect

		Model	Ship	
Full Load	Sagging	80.0 in.-lb.	237,500	ton-meters
	Hogging	38.7 in.-lb.	115,000	"
Ballast	Sagging	52.9 in.-lb.	157,000	"
	Hogging	54.5 in.-lb.	161,800	"

3. Measured Model and Ship Characteristics:

a. Radius of gyration	Model	Ship
Full Load	0.212 L.B.P.	0.221 L.B.P.
Ballast	0.223 L.B.P.	

b. Natural pitching period	Model
Full Load	0.69 seconds
Ballast	0.64 seconds

c. Actual natural frequency of vertical two-noded vibration

	Model
Full Load	10.5 c.p.s.
Ballast	10.0 c.p.s.

4. Loading of the Model and Ship:

a. These model loadings were followed as closely as possible in the tests. The model sections are as follows:

Section 1 is the sternmost section from station 8 to the stern;

Section 2 is the six inch section forward of section 1,

from station 10 to station 8;

Section 3 is the six inch section forward of section 2, from station 12 to station 10;

Section 4 is the bow from station 12 forward.

b. Loadings:

Section	Ship		Model		
	Weight (Metric tons)	Long. Arm (Meters)	Weight (Pounds)	Long. Arm (Inches)	Long. Arm taken about Section
1. Full Load Condition No. 11:					
1	14,280	26.33	15.32	8.22	8
2	6,275	8.76	6.73	2.74	10
3	5,381	11.82	5.79	3.69	10
4	16,518	28.22	17.76	8.22	12
	42,454		45.60		
2. Ballast Condition No. 4:					
1	10,305	27.93	11.10	8.73	8
2	3,504	9.05	3.77	2.83	10
3	3,003	12.75	3.23	3.98	10
4	11,043	26.23	11.90	8.20	12
	27,855		30.00		

APPENDIX B

Sample Calculations

1. Determination of Radius of Gyration:

a. The model was suspended by two springs of equal spring constant at equal distances from the center of gravity and made to oscillate in air, first in pitching, then in heaving. The time for 30 cycles for each was taken by stop watch. The following formula then gave the radius of gyration.

$K_y = (T_p/T_h)l$

K_y = radius of gyration in inches, or as a fraction of L.B.P.

T_p = pitching period in air in seconds

T_h = heaving period in air in seconds

l = distance from springs to the center of gravity in inches = 29.0 inches

b. Full Load:

$T_p = 0.285 \times 60/30 \qquad T_h = 0.65 \times 60/30$

$K_y = (0.285/0.65)29.0 = 12.7$ inches $= K_y$

$K_y = \frac{12.7}{60} \qquad \underline{K_y = 0.212 \text{ L.P.B.}}$

c. Ballast:

$T_p = 0.245 \times 60/30 \qquad T_h = 0.53 \times 60/30$

$K_y = (0.245/0.53)29.0 = 13.4$ inches $= K_y$

$K_y = \frac{13.4}{60} \qquad \underline{K_y = 0.223 \text{ L.B.P.}}$

2. Determination of the Natural Period of the Vertical Two-Noded Vibration of the Ship.

a. The modified Schlick formula was used for this calculation as follows:

$$N = \frac{\phi}{\sqrt{(1 + B/2d)(1 + r)}} \times \sqrt{\frac{I}{\Delta L^3}}$$

N = frequency, c.p.m.
I = midship section moment of inertia in feet^4
Δ = displacement in tons
L = L.B.P. in feet
B = Beam in feet
d = draft in feet
D = molded depth in feet
a = B/D
ϕ = 2,400,000

$$r = \frac{3.5\,D^2(3a^3 + 9a^2 + 6a + 1.2)}{L^2\,(3a + 1)}$$

$a = B/D = 89.01/45.21 = 1.968$

$a^2 = 3.87 \quad a^3 = 7.62$

$$r = \frac{3.5(45.21)^2(3 \times 7.62 + 9 \times 3.87 + 6 \times 1.968 + 1.2)}{(630.0)(630.0)(3 \times 1.968 + 1)} = r = 0.185$$

b. <u>For Full Load</u>:

$$N = \frac{2,400,000}{\sqrt{1 + 89.01/67.7)(1.185)}} \times \sqrt{\frac{13,489}{41,785(630.0)^3}}$$

$N = 52.2$ cycles/minute $= 0.870$ cycles/second

For the model then:

$N = 0.870\sqrt{126} = 9.76$ cycles/second

c. <u>Similarly for the Ballast Condition</u>:

$N = 57.1$ cycles/minute $= 0.952$ cycles/second

For the model:

$N = 0.952 \times 11.22 = 10.7$ cycles/second

3. <u>Calculation of the Aluminum Flexure Bar Size to give the proper Vertical Two-Noded Vibration Frequency to the Model</u>.

From Reference (10) the added water mass is obtained:

$M = \frac{1}{2}\ CJ\pi B^2 \rho g = \text{lb./ft.}$

$B = \frac{1}{2}$ breadth $= 0.353$ ft.

$\rho g =$ water density, lb./cu.ft.

from curves with $L/B = 0.708$, $J = 0.78$

$B/d = \frac{44.5}{33.85} = 1.314$; then from curves $C = 1.4$

$M = \frac{1}{2} \times 1.4 \times 0.78 \times (0.353)^2 \times 62.4 =$

$M = 13.3$ lb./ft.

$$K.E. = \sum \frac{W}{2g} w^2 x^2 + \sum \frac{J}{2g} w^2 \theta^2$$

$$P.E. = \frac{EI\phi^2}{2h}$$

Assumed deflected shape of the flexure bar

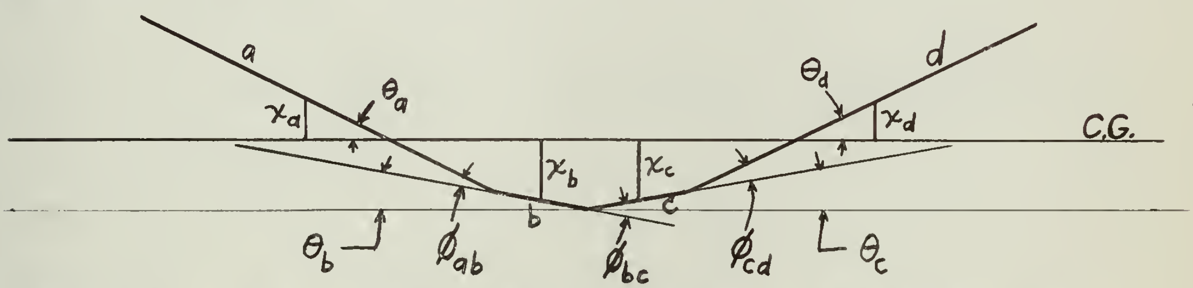

Section	θ	x(ft)	W(lb)	M(lb)	W + M(lb)	ϕ
a	0.2269	0.046	18.71	26.6	45.3	
						0.1396
b	0.0873	0.1833	4.68	6.65	11.33	
						0.1745
c	0.0873	0.1833	4.68	6.65	11.33	
						0.1396
d	0.2269	0.046	18.71	26.6	45.3	

P.E. = Potential Energy in foot-pounds

K.E. = Kinetic Energy in foot-pounds

h = unsupported length of bar = 3 inches = 0.25 feet

W = weight in pounds

w = circular frequency in radians per second

x = displacement in feet

J = polar moment of inertia in pounds-feet^2

θ and ϕ are angles as shown on diagram in radians

I = moment of inertia of the bar in. feet^4

E = modulus of elasticity = 10,000,000 p.s.i. for aluminum

$J = WL^2/12$ for a, $J = 45.3 \times 4/12 = 15.1$ lb.ft.^{2}

for b, $J = 11.33 \times 0.25/12 = 0.236$ lb.ft.^{2}

$$KE = 2w^2(0.046)^2 \times 45.3/64.4 + 2w^2(0.1833)^2 \times 11.33/64.4 + 2w^2(.227)^2 \times 15.1/64.4 + 2w^2(0.0873)^2 \times 0.236/64.4$$

$$KE = 0.03908w^2$$

$$PE = 2 \times 144 \times 10^7 \times I \times (.1396)^2/0.5 + 144 \times 10^7 \times I \times (0.1745)^2/0.5$$

$$PE = 2 \times 10^8\ I$$

$$PE = KE \qquad 0.03908w^2 = 2 \times 10^8\ I$$

The highest frequency of encounter $\approx$ 1.6 c.p.s., therefore make the natural frequency of vibration $5 \times 1.6 = 8$ c.p.s.; then $w = 2\pi f = 16\pi = 50.3$ $\quad w^2 = 2530$

$$I = \frac{0.03908}{2 \times 10^8} \times 2530 \times 144 \times 144 = 0.01026 \text{ inches}^4$$

$$I = \frac{bt^3}{12} \qquad \text{if } b = 1 \text{ inch, } t^3 = 12 \times 0.01026$$

$$t = \sqrt[3]{0.1231} = 0.498 \text{ inches}$$

So we used an aluminum bar 1 inch wide by 1/2 inch thick to give a natural frequency of vertical two-noded vibration of 8.0 cycles per second.

APPENDIX C

Drawings and Photographs

FIGURE XV

Drawing of Model Showing Flexure Bar Location

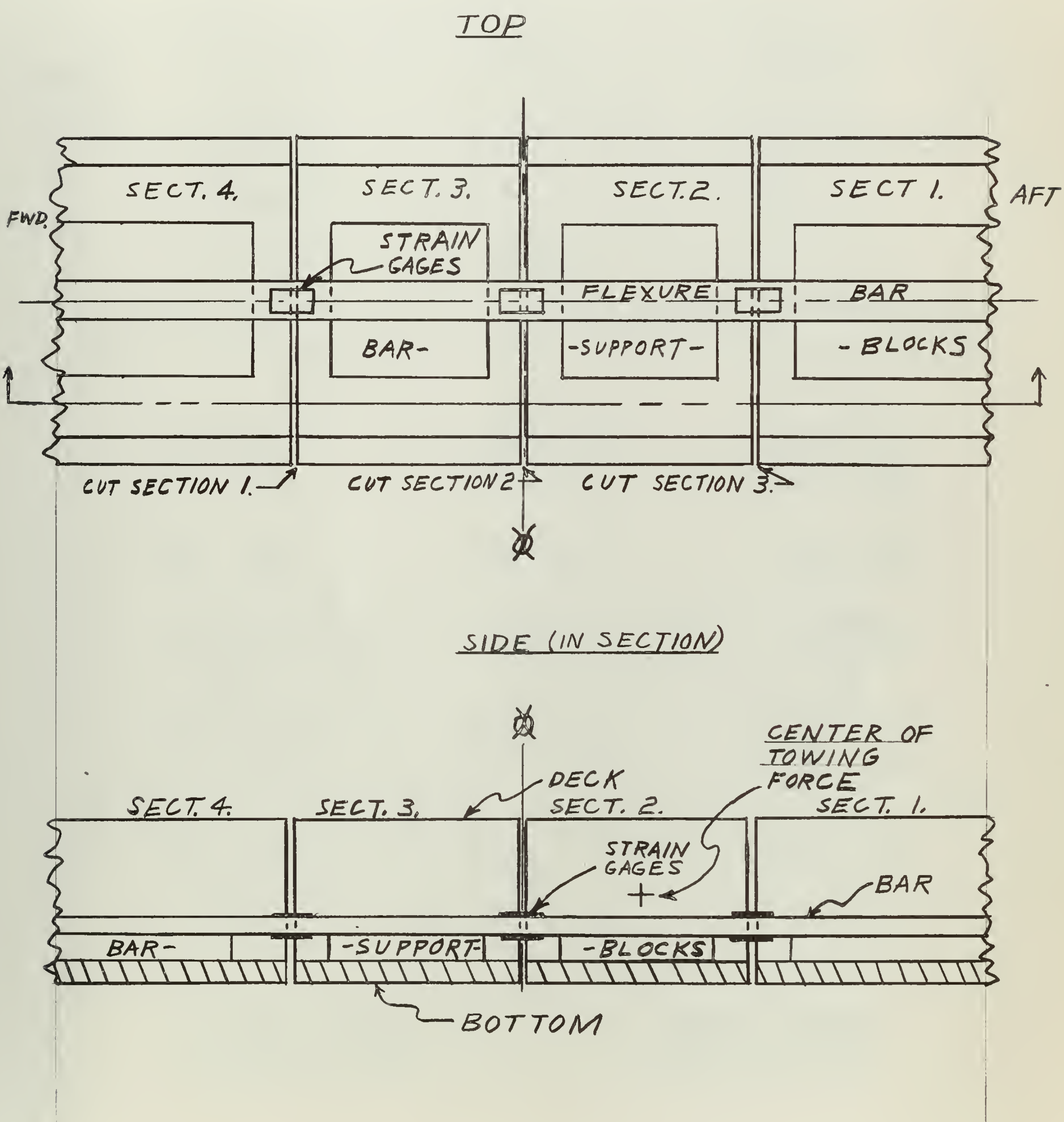

FIGURE XVI

Diagrams of Strain Gage Installations

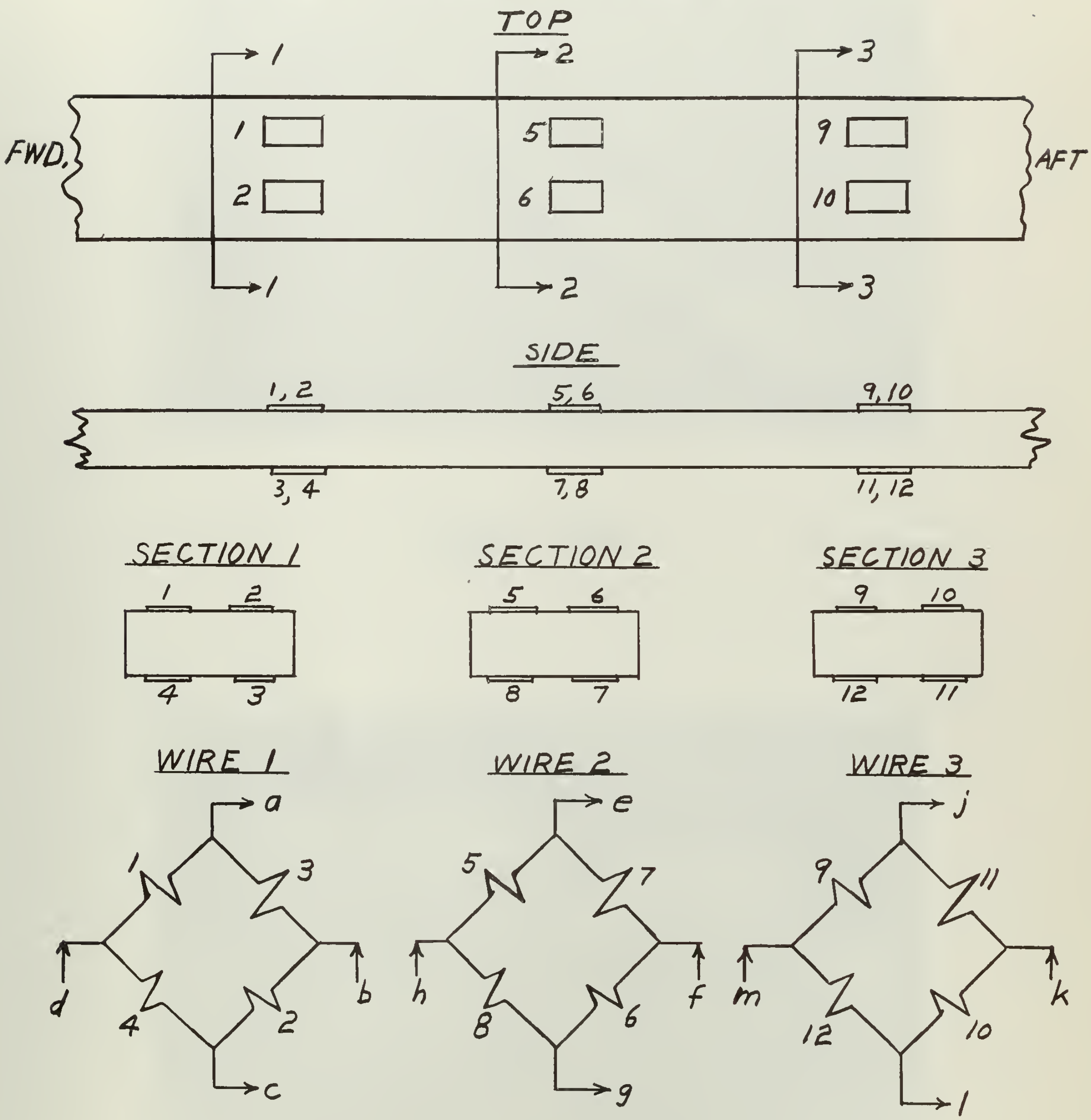

OUTPUT LEADS:
a, c, e, g, j, l.

INPUT LEADS:
b, d, f, h, k, m.

Figure XVII

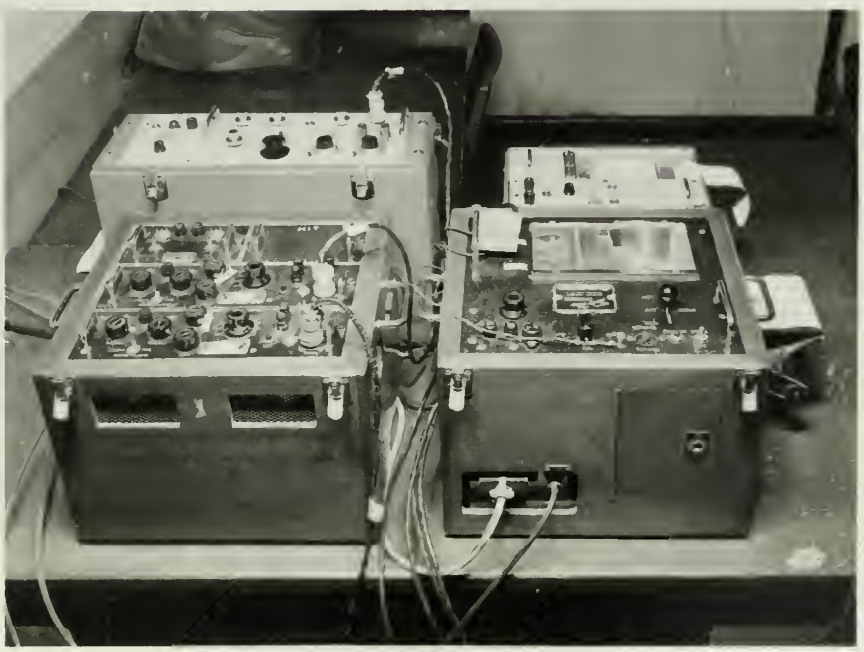

Figure XVIII

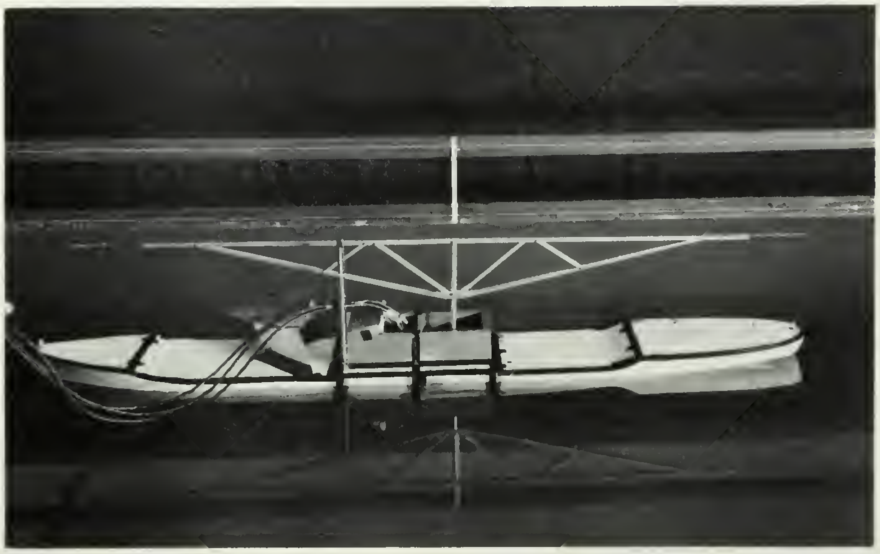

Figure XIX

Figure XX

Figure XXI

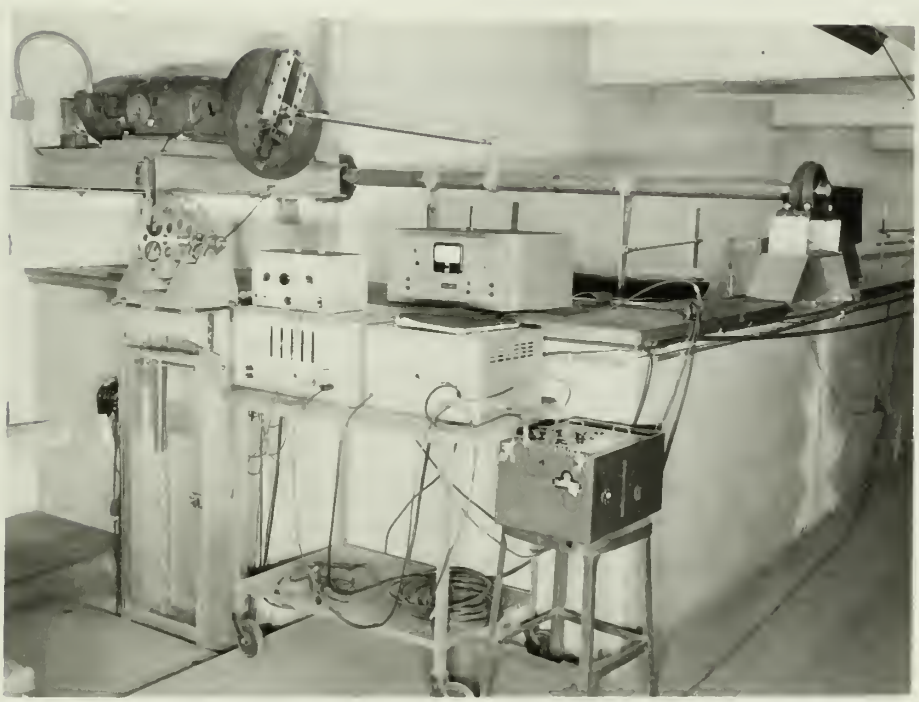

Figure XXII

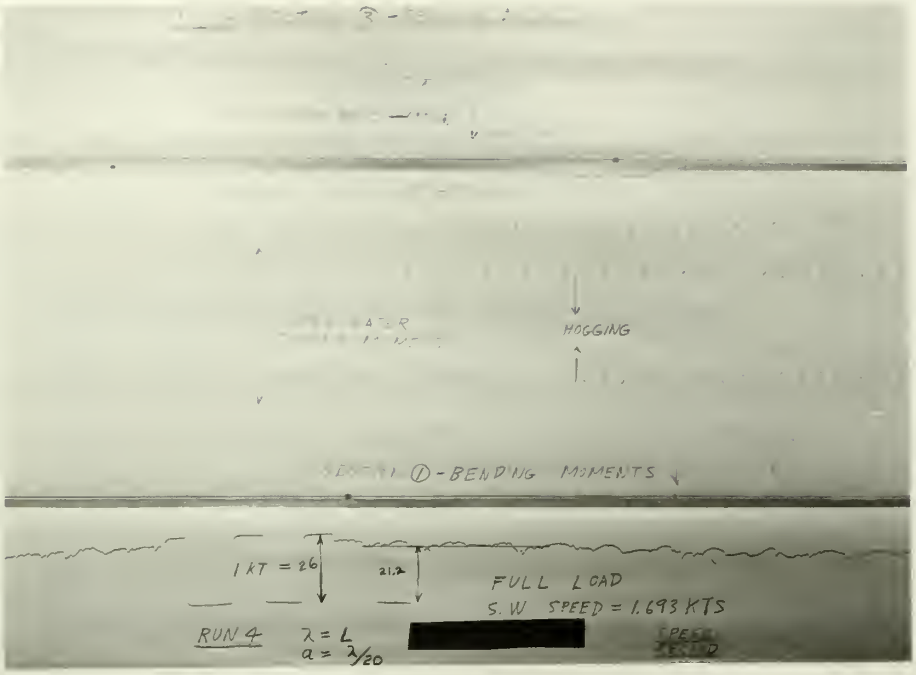

Figure XXIII

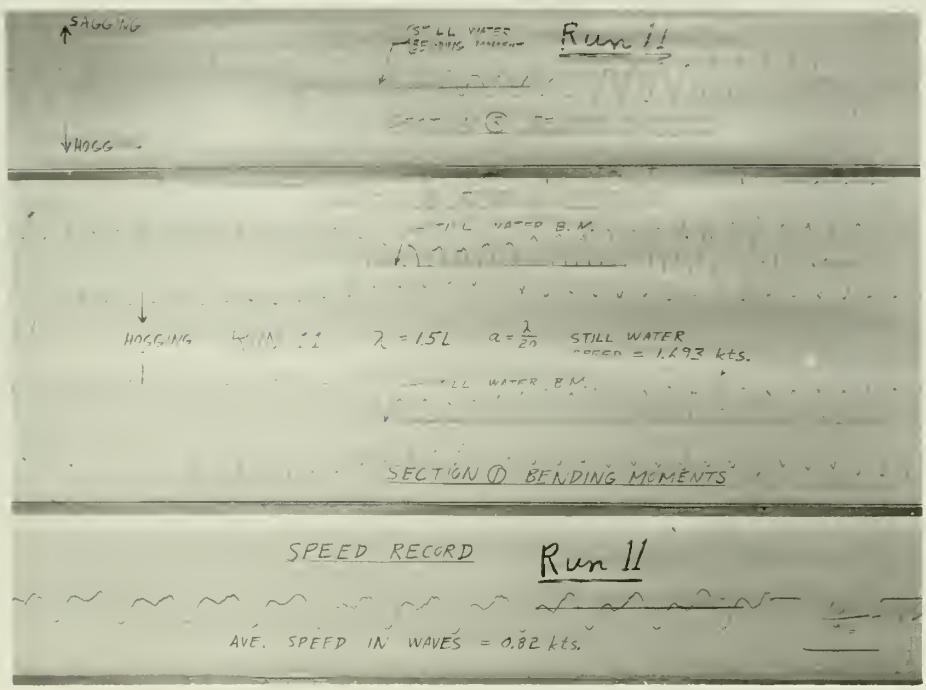

Figure XXIV

APPENDIX D

Original Data

TABLE I

Original Data

Still Water Speeds and Towing Forces

Full Load Condition

Tow force - lbs.	Vs. of ship - kts.	Vs. of model - kts.
0.080	9.9	0.881
0.110	11.9	1.061
0.200	16.6	1.478
0.300	19.0	1.693

Ballast Condition

Tow force - lbs.	Vs. of ship - kts.	Vs. of model - kts.
0.070	10.1	0.900
0.100	12.1	1.077
0.180	16.3	1.456
0.250	18.4	1.639

[illegible]

[illegible]

[illegible]

[illegible]

[illegible]	[illegible]	[illegible]	[illegible]	[illegible]	[illegible]
	[illegible]				[illegible]
	[illegible]		[illegible]		[illegible]
	[illegible]		[illegible]		[illegible]
	[illegible]		[illegible]		[illegible]

[illegible]

[illegible]	[illegible]	[illegible]	[illegible]	[illegible]	[illegible]
	[illegible]				[illegible]
	[illegible]		[illegible]		[illegible]
	[illegible]				[illegible]
	[illegible]		[illegible]		[illegible]

TABLE II

Original Data

Zero Speed Bending Moments (in.-lbs.)

Full Load Condition

Run No.	λ/L	Forward Section Hog	Forward Section Sag	Midship Section Hog	Midship Section Sag	Aft Section Hog	Aft Section Sag
A	1	18.9	26.5	24.2	33.3	21.1	29.8
B	0.75	15.0	16.3	13.0	24.2	13.3	16.8
C	0.75	11.5	12.0	13.0	18.2	11.9	14.7
D	1.25	27.4	36.8	26.7	37.0	21.8	33.3

Ballast Condition

Run No.	λ/L	Forward Section Hog	Forward Section Sag	Midship Section Hog	Midship Section Sag	Aft Section Hog	Aft Section Sag
A'	1	22.1	31.9	20.9	31.8	20.7	20.7
B'	1.5	25.8	30.7	22.4	34.5	26.5	36.8
C'	0.75	13.1	20.0	12.1	18.2	12.0	17.9
D'	0.5	7.4	8.2	4.2	4.8	1.8	2.1

All wave heights = $\lambda/20$ except for Run B where $\lambda = \frac{L}{20}$

[illegible]

[illegible]

[illegible]

[illegible]

[illegible]	[illegible]	[illegible]	[illegible]	[illegible]	[illegible]	[illegible]
[illegible]	[illegible]	[illegible]	[illegible]	[illegible]		
[illegible]	[illegible]			[illegible]		
[illegible]	[illegible]	[illegible]	[illegible]	[illegible]	[illegible]	
[illegible]	[illegible]	[illegible]	[illegible]	[illegible]	[illegible]	

[illegible]

[illegible]	[illegible]	[illegible]	[illegible]	[illegible]	[illegible]	[illegible]	[illegible]
[illegible]	[illegible]	[illegible]	[illegible]	[illegible]	[illegible]	[illegible]	
[illegible]	[illegible]	[illegible]	[illegible]	[illegible]	[illegible]	[illegible]	
					[illegible]		[illegible]

[illegible]

TABLE III

Original Data

Speeds in Waves for Full Load Condition - Wave Height = $\lambda/20$

Run No.	λ/L	Vs (kts.)	Vv (kts.)
3	1	1.478	0.72
4	1	1.693	0.85
5	1	1.061	.28
6	1	0.881	.15
7	.75	0.881	
8	.75	1.061	
9	.75	1.693	
10	.75	1.478	
11	1.5	1.693	.82
12	1.5	1.478	.63
13	1.5	1.061	.53
14	1.5	0.881	.45
15	.75	1.478	.48
16	.75	1.061	.20
17	.75	0.881	.05
18	.75	1.693	1.00
19	.4	0.881	0.79
20	.4	1.061	
21	.4	1.478	1.47
22	.4	1.693	1.59

[illegible]

[illegible]

[illegible]	[illegible]	[illegible]	[illegible]
[illegible]			
[illegible]	[illegible]		
	[illegible]		
[illegible]	[illegible]	[illegible]	
	[illegible]	[illegible]	
	[illegible]		
	[illegible]	[illegible]	[illegible]
	[illegible]		
[illegible]	[illegible]	[illegible]	[illegible]
[illegible]	[illegible]	[illegible]	[illegible]
[illegible]	[illegible]	[illegible]	[illegible]
[illegible]	[illegible]		[illegible]
[illegible]	[illegible]	[illegible]	[illegible]
[illegible]	[illegible]	[illegible]	[illegible]
[illegible]	[illegible]		
[illegible]	[illegible]	[illegible]	[illegible]
[illegible]	[illegible]		
	[illegible]	[illegible]	[illegible]
[illegible]	[illegible]	[illegible]	[illegible]
[illegible]	[illegible]		

TABLE IV

Original Data

Dynamic Bending Moments (in.-lbs.) for Full Load Condition - Wave Height = λ/20

Run No.	Forward Section Hog	Forward Section Sag	Midship Section Hog	Midship Section Sag	Aft Section Hog	Aft Section Sag
3	21.6	33.8	29.6	37.9	27.4	38.3
4	27.2	30.1	33.6	34.8	26.3	26.3
5	28.5	28.0	34.8	38.5	23.2	38.3
6	24.6	34.3	30.6	38.5	22.5	33.7
7	23.9	18.8	20.0	26.9	15.4	23.4
8	23.0	23.2	22.4	30.0	17.6	23.4
9	23.0	20.4	25.3	22.9	19.7	17.8
10	22.3	22.5	20.3	26.6	15.8	19.3
11	37.3	45.8	43.0	53.6	28.1	40.4
12	31.7	35.7	33.0	45.5	21.4	32.6
13	31.5	41.9	38.5	43.6	25.3	35.8
14	31.7	38.4	36.1	47.0	24.6	34.7
15					25.6	35.8
16	20.7	25.8	22.1	30.0	14.7	23.4
17	21.2	22.3	20.3	27.0	15.8	17.9
18	23.0	28.1	24.5	29.7	14.0	27.0
19	No data					
20	No data					
21	5.5	5.5	5.3	5.3	4.1	3.6
22	4.6	4.6	4.2	4.2	2.8	3.6

TABLE V

Original Data

Speeds in Waves for Ballast Condition - Wave Height = $\lambda/20$

Run No.	λ/L	Vs (kts.)	Vv (kts.)
31	1	1.077	.34
32	1	.900	.30
33	1	1.456	.59
34	1	1.639	.82
35	1.5	1.639	1.00
36	1.5	1.456	.74
37	1.5	1.077	.52
38	1.5	.900	.47
39	0.75	.900	.31
40	0.75	1.077	.56
41	0.75	1.456	.75
42	0.75	1.639	.89
43	0.5	1.639	1.60
44	0.5	1.456	1.32
45	0.5	1.077	.51
46	0.5	.900	.31
47	1	1.639	
48	1	1.456	
49	1	1.077	
50	1.5	1.639	
51	1.5	1.456	
52	1.5	1.077	

TABLE VI

Original Data

Dynamic Bending Moments (in.-lbs.) for Ballast Condition - Wave Height = $\lambda/20$

Run No.	Forward Section Hog	Forward Section Sag	Midship Section Hog	Midship Section Sag	Aft Section Hog	Aft Section Sag
31	29.9	31.5	25.5	30.6	24.2	30.6
32	26.6	33.1	27.3	30.9	20.5	34.0
33	27.0	30.7	22.7	32.7	29.4	37.3
34	39.7	31.1	27.0	37.6	27.6	36.8
35	29.0	43.4	24.5	39.7	27.8	36.8
36	24.1	32.7	19.4	31.2	19.8	24.2
37	31.9	32.3	26.4	36.4	32.7	31.3
38	29.0	31.5	28.8	32.7	27.4	33.6
39	14.6	18.0	10.0	17.3	-25.5- range	
40	21.7	22.1	18.2	21.2	41.9	"
41	22.1	22.9	15.2	23.0	29.9	"
42	21.2	24.5	20.6	16.4	34.5	"
43	9.0	9.0	4.8	4.8		
44	No data					
45	No data					
46	No data					
47	29.8	36.5	22.8	29.0		
48	26.5	33.0	20.8	29.0		
49	24.0	31.3	25.0	29.0		
50	19.5	29.8				
51	22.7	36.8	15.0	27.4		
52	26.3	32.0	25.0	29.0		

Thesis 35896
L94 Lutzi
Ship model bending moments
in waves.